AFML-TR-77-95

12

THE EFFECT OF HYDRAZINE DECOMPOSITION PRODUCTS ON THE MECHANICAL PROPERTIES OF HIGH-TEMPERATURE ALLOYS

ROCKETDYNE DIVISION
ROCKWELL INTERNATIONAL
6633 CANOGA AVENUE
CANOGA PARK, CALIFORNIA 91304

15 MARCH 1978

TECHNICAL REPORT AFML-TR-77-95
Final Report for Period 1 March 1976 to 1 April 1977

Approved for public release; distribution unlimited.

AIR FORCE MATERIALS LABORATORY
AIR FORCE WRIGHT AERONAUTICAL LABORATORIES
AIR FORCE SYSTEMS COMMAND
WRIGHT-PATTERSON AIR FORCE BASE, OHIO 45433

NOTICE

This report has been reviewed by the Information Office (OI) and is releasable to the National Technical Information Service (NTIS). At NTIS, it will be available to the general public, including foreign nations.

This technical report has been reviewed and is approved for publication.

Norman M Geyer

NORMAN M. GEYER
Project Engineer
High Temperature Materials Group

FOR THE COMMANDER

Norman M Tallan

NORMAN M. TALLAN
Chief, Processing and High Temperature
 Materials Branch
Metals and Ceramics Division
Air Force Materials Laboratory

AIR FORCE/56780/26 January 1978 — 300

UNCLASSIFIED

SECURITY CLASSIFICATION OF THIS PAGE (*When Data Entered*)

(18) (19) **REPORT DOCUMENTATION PAGE**

READ INSTRUCTIONS BEFORE COMPLETING FORM

1. REPORT NUMBER
AFML-TR-77-95✓

(9) Final rept. 1 Mar 76-1 Apr 77,

4. TITLE (and Subtitle)
(6) The Effect of Hydrazine Decomposition Products on the Mechanical Properties of High-Temperature Alloys

5. TYPE OF REPORT & PERIOD COVERED
Final (1 March 1976 to 1 April 1977)

(14) 6. PERFORMING ORG. REPORT NUMBER
RI/RD77-143✓

7. AUTHOR(s)
(10) W. T. Chandler

(15) 8. CONTRACT OR GRANT NUMBER(s)
F33615-76-C-5201 new
(CLIN 00001, Seq. 2)

9. PERFORMING ORGANIZATION NAME AND ADDRESS
Rocketdyne Division of Rockwell International✓
6633 Canoga Avenue
Canoga Park, California 91304

10. PROGRAM ELEMENT, PROJECT, TASK AREA & WORK UNIT NUMBERS (16) (17)
62102F, 7312, 731202
73120224

11. CONTROLLING OFFICE NAME AND ADDRESS
Air Force Materials Laboratory
Air Force Systems Command
Wright Patterson AFB, Ohio 45433

(11) 12. REPORT DATE
15 MAR 78

(12) 13. NUMBER OF PAGES
63 p.

14. MONITORING AGENCY NAME & ADDRESS (*if different from Controlling Office*)

15. SECURITY CLASS. (*of this report*)
Unclassified

15a. DECLASSIFICATION/DOWNGRADING SCHEDULE

16. DISTRIBUTION STATEMENT (*of this Report*)
Approved for public release;
distribution unlimited.

17. DISTRIBUTION STATEMENT (*of the abstract entered in Block 20, if different from Report*)

18. SUPPLEMENTARY NOTES

19. KEY WORDS (*Continue on reverse side if necessary and identify by block number*)
Haynes 188, Inconel 600, Rene' 41, IN-100
Hydrazine decomposition products
High-pressure ammonia, nitrogen, and hydrogen
Low-cycle fatigue
Tensile properties
Scanning electron fractography

20. ABSTRACT (*Continue on reverse side if necessary and identify by block number*)

An experimental and analytical program was conducted to develop data for the screening and selection of alloys for use in APU system gas generator and turbine components, where such components are exposed to environmental effects of hydrazine decomposition products. Alloys selected for investigation were Haynes 188 and Inconel 600 as candidates for the gas generator, and Rene' 41 and IN-100 as candidates for turbine components. Tension tests and compressive low-cycle fatigue tests were performed on hollow specimens pressurized internally with 700-psi $NH_3/N_2/H_2$ gas mixtures simulating APU hydrazine decomposition products and with

over

DD FORM 1 JAN 73 1473 EDITION OF 1 NOV 65 IS OBSOLETE

UNCLASSIFIED

SECURITY CLASSIFICATION OF THIS PAGE (*When Data Entered*)

390 199

20.

argon for comparison. Test temperatures were 1450 and 1600 F, with other test parameters selected to be pertinent to advanced APU technology. There was no significant difference in the tensile properties between specimens exposed to the $NH_3/N_2/H_2$ gas mixtures and those exposed to argon for any of the materials. The low-cycle fatigue life was slightly reduced by the $NH_3/N_2/H_2$ environments for Haynes 188 and for Inconel 600 at a high strain range, but no effect was found for Rene' 41 or IN-100.

PREFACE

This report was prepared by the Rocketdyne Division, Rockwell International, Canoga Park, California 91304, under Air Force Contract F33615-76-C-5201, and represents a final technical report covering the period 1 March 1976 through 1 April 1977. The contract was administered by the Metals and Ceramics Division, Air Force Materials Laboratory, Air Force Systems Command, Wright-Patterson Air Force Base, Ohio, with Mr. N. M. Geyer (AFML/LLM) as Project Engineer.

Dr. J. R. Lewis was the Rocketdyne Project Manager and Dr. W. T. Chandler was the Principal Investigator. Acknowledgment is gratefully given to the following for their contributions to this investigation: Dr. A. J. Jacobs (now at General Electric Nuclear Energy Division, San Jose, California), who was Principal Investigator at the initiation of the program; Messrs. A. F. Konigsfeld, R. S. Kennedy, and R. M. Parker, who set up the test system and performed the tests; Ms. Rebecca Richards (Rockwell International Science Center), who performed the scanning electron fractography, and Mr. R. J. Walter, who assisted in interpreting the electron fractographs.

TABLE OF CONTENTS

PrecedING Page BLANK

LIST OF ILLUSTRATIONS

LIST OF TABLES

SUMMARY

A program was conducted to determine the effect of $NH_3/N_2/H_2$ environments simulating APU system hydrazine decomposition products on the properties of Haynes 188, Inconel 600, Rene' 41, and IN-100. Tension and low-cycle fatigue tests were performed on hollow specimens pressurized internally with 700-psi $NH_3/N_2/H_2$ gas mixtures or with argon for comparison. The $NH_3/N_2/H_2$ tension tests were performed at 1450 F with and without a 2-hour hold period with the environment prior to tension testing. Tests were also performed at 1600 F after 2-hour hold periods. Argon tension tests were performed at 1450 F with no hold period. Cross sections of selected tension-tested specimens were examined by optical microscopy. The low-cycle fatigue tests were strain-cycling tests with a sawtooth, compressive cycle at a frequency of 0.5 Hz. The low-cycle-fatigue tests were conducted at 1450 F at two strain ranges, approximately 1.5 and 0.8%. The fracture surfaces of selected low-cycle-fatigue specimens were examined by scanning electron microscopy. There was no significant difference in the tensile properties between specimens exposed to the $NH_3/N_2/H_2$ gas mixtures and those exposed to argon for any of the materials. The low-cycle-fatigue life was slightly reduced by the $NH_3/N_2/H_2$ environments for Haynes 188 and for Inconel 600 at a high strain range, but no effect was found for Rene' 41 or IN-100.

INTRODUCTION

Auxiliary power units (APU's) to provide hydraulic and electrical power for various purposes are currently under intensive development, especially for high-power airborne device requirements. The monopropellant type of APU has the important advantage of the fuel being storable. Hydrazine (N_2H_4) is one of the most widely used and best-characterized monopropellants. It has a relatively high energy and is virtually carbon-free, so that contamination from this source is minimal.

Energy is provided by the decomposition of the hydrazine in either a catalytic or thermal monopropellant reactor situated upstream from a turbine. The decomposition of the hydrazine is strongly exothermic and produces ammonia, nitrogen, and hydrogen. Depending on reactor geometry, some of the ammonia that is formed may decompose on metal surfaces downstream and, since this reaction is endothermic, the exhaust gas temperatures will be lower than those resulting from the initial hydrazine decomposition. The dissociation of ammonia produces atomic hydrogen and nitrogen.

The ammonia that decomposes is a powerful nitriding agent (Ref. 1). This is because nitrogen atoms are strongly chemisorbed on some metal surfaces, and there is a small activation energy involved in the chemisorption process from ammonia, while a large activation energy is involved in the case of molecular nitrogen. The adsorbed nitrogen atoms may be readily absorbed into the metal (Ref. 2) and they either dissolve or form nitrides by reaction with various constituents that may be present.

Nickel-base and cobalt-base alloys are the main candidates for use in reactors and turbines in hydrazine-based APU's because of their high-temperature strength and ductility. However, the use of these alloys

---

Ref. 1. Kindlimann, L. E., and G. S. Ansell: Met. Trans., 1, 163 (1970).

Ref. 2. Nitriding Processes, Bulletin No. AP-1, 21 pages, Armour Industrial Nitrogen Division, Atlanta, GA., 1967.

might pose a compatibility problem, since the very constituents that contribute to solid-solution hardening or precipitation hardening are strong nitride formers. Nitride formation from aluminum, titanium, molybdenum, tungsten, columbium, boron, and zirconium is feasible both thermodynamically and kinetically at the temperatures and durations appropriate to hydrazine gas generator technology. Chromium, which is added to the nickel and cobalt families of alloys for improving oxidation resistance, is also subject to nitriding.

Three hydrogen-related problems that might limit the use of nickel and cobalt alloys in hydrazine APU's are hydrogen-reaction embrittlement, internal hydrogen embrittlement, and hydrogen-environment embrittlement (HEE). The first two problems (Ref. 3 through 9) have been recognized

---

Ref. 3. Smith, D. P.: Hydrogen in Metals, University of Chicago Press, Chicago, Illinois (1948).

Ref. 4. Buzzard, R. W., and H. E. Cleaves: Hydrogen Embrittlement of Steel: Review of the Literature, National Bureau of Standards Circular 511 (1951).

Ref. 5. Smialowski, M.: Hydrogen in Steel, Pergamon Press, Ltd., Addison-Wesley Publishing Company, Reading Massachusetts (1962).

Ref. 6. Fletcher, E. E., and A. R. Elsea: The Effects of High-Pressure High-Temperature Hydrogen on Steel, DMIC Report 202, Defense Metals Information Center, Battelle Memorial Institute, Columbus, Ohio (26 March 1964).

Ref. 7. Groeneveld, T. P., E. E. Fletcher, and A. R. Elsea: Review of Literature on Hydrogen Embrittlement, Special Report on Contract NAS8-20029, NASA, MSFC, Huntsville, Alabama, 12 January 1966.

Ref. 8. Tetelman, A. S.: The Mechanism of Hydrogen Embrittlement in Steel, Fundamental Aspects of Stress Corrosion Cracking, National Association of Corrosion Engineers, Houston, Texas, p. 446 (1969).

Ref. 9. Bernstein, I. M.: "The Role of Hydrogen in the Embrittlement of Iron and Steel," Materials Science and Engineering, 6, 1 (1970).

and studied for much longer time than hydrogen-environment embrittlement (Ref. 10 through 13). Hydrogen-reaction embrittlement can result, for example, from the formation of an embrittling hydride (e.g., titanium hydride) or of high-pressure gas pockets as the result of reaction of the hydrogen with oxygen to form water vapor or with carbon to form methane. Internal hydrogen embrittlement is due to hydrogen absorbed into and throughout the metal. The best recognized example of this embrittlement is the delayed failure of hydrogen-charged, high-strength steels. Hydrogen reactions and absorption of hydrogen from the gas are accelerated by elevated temperatures. The third problem is normally manifested while a metal or alloy (nickel and cobalt alloys are in this category) is stressed in high-pressure hydrogen. A specimen exposed to high-pressure hydrogen, then tested in air, does not show the effect. Furthermore, HEE in molecular hydrogen is usually a maximum near-ambient temperature; whereas, when atomic hydrogen is available, HEE becomes a serious problem over a broad temperature range (Ref. 14). The presence of a nitride on a metal surface naturally would complicate the processes of ammonia decomposition and hydrogen interaction with the metal.

Ref. 10. Walter, R. J., and W. T. Chandler: *Effects of High-Pressure Hydrogen on Storage Vessel Materials*, Paper presented at 1968 Western Metal and Tool Conference, Los Angeles, California, March 1968. ASM Report No. W8-2-4, ASM Report System, Metals Park, Ohio, 44073.

Ref. 11. Walter, R. J., and W. T. Chandler: *Effects of High-Pressure on Metals at Ambient Temperature*, Final Report, Contract NAS8-19, NASA, MSFC, Huntsville, Alabama, Rocketdyne, a division of North American Rockwell, Canoga Park, California, Report R-7780-1, -2, -3, 1969.

Ref. 12. Walter, R. J., R. P. Jewett, and W. T. Chandler: "On the Mechanism of Hydrogen-Environment Embrittlement of Iron and Nickel-Base Alloys," *Materials Science and Engineering*, *5*, 98 (1969/1970).

Ref. 13. Jewett, R. P., R. J. Walter, W. T. Chandler, and R. P. Frohmberg: *Hydrogen-Environment Embrittlement of Metals*, a NASA Technology Survey, NASA CR-2163, March 1973.

Ref. 14 Nelson, H. G., D. P. Williams, and A. S. Tetelman: *Met. Trans.*, *2*, 953 (1971).

In summary, the decomposition of hydrazine and the subsequent decomposition of ammonia results in a gas mixture of ammonia, hydrogen, and nitrogen, any of which might cause the degradation of mechanical properties of metals of interest for use in gas generators and turbines. Little data exist that can be used to select metals able to meet the demanding requirements of operating stresses, temperatures, and cycles in this environment.

Thus, this program was conducted to determine the effect of exposure to hydrazine decomposition products on the mechanical properties of four selected nickel-base and cobalt-base alloys. Tension and low-cycle fatigue tests were conducted with specimens exposed to gas mixtures typical of hydrazine decomposition products at temperatures, pressure, and exposure times pertinent to hydrazine APU technology.

EXPERIMENTAL PROCEDURES

ALLOY SELECTION AND PROCUREMENT

The alloys selected and approved by the Air Force project engineer for investigation under this program were Haynes 188, Inconel 600, Rene' 41, and IN-100. Haynes 188 and Inconel 600 are candidates for the gas generator; the other two alloys are for the turbine. The compositions for these alloys are listed in Table 1. The compositions of all alloys are from vendor-certified analyses. Table 2 contains the applicable specifications for the alloys and the form in which they were procured.

The alloys were selected with two objectives in mind. The first, short-range objective was to obtain data for predicting the performance of the current hydrazine-fueled, flight-type gas generator (GG) (Rocketdyne Air Force Subcontract 419-56002-5 to AiResearch) and the fast-start turbine (Air Force Contract F33615-74-C-2013). The second objective was more general and long range in scope. This objective was to lay a foundation for rational (nonempirical) alloy selection by correlating the test data with composition and microstructure, and identifying the key features in the failure mechanisms. Nitrogen and/or hydrogen embrittlement were expected to play some role in these mechanisms.

Three (Haynes 188, Inconel 600, and Rene' 41) of the four selected alloys will be used in the first-generation hardware. Haynes 188 is Co-base and high (37.1%) in content of nitride-forming elements (see Table 1). Rene' 41 is Ni-base and also high (34.0%) in nitride formers. The Ni-base Inconel 600 is low (15.6%) in nitride formers. The fourth alloy, Ni-base IN-100, was chosen for three reasons: (1) it is a candidate for future turbine designs, (2) it is a cast alloy offering net-shape cost advantages, and (3) it represents an intermediate composition (23.5% nitride formers) between those of Inconel 600 and Rene' 41. Thus, it would be possible to compare a Co-base alloy with a Ni-base alloy,

TABLE 1. COMPOSITIONS OF ALLOYS SELECTED FOR INVESTIGATION

Alloy	C	Mn*	Si*	Cr*	Ni	Co	Mo*	W*	Cb*	Ti*	Al*	B*	Zr*	Fe	Cu	S	Other	% Nitride Formers
Haynes 188	0.08	0.74	0.34	22.00	22.20	Bal.	-	13.95	-	-	-	-	-	1.96	-	0.006	La*004	37.1
Inconel 600	0.07	0.38	0.14	15.04	74.61	-	-	-	-	-	-	-	-	9.44	0.31	0.006	-	15.6
Rene'41	0.09	0.10	0.10	18.8	Bal.	10.9	10.2	-	-	3.25	1.52	0.010 Max.	-	0.71	-	0.003	-	34.0
IN-100	0.20	0.02	0.03	10.58	Bal.	15.23	3.07	-	-	[illegible].24	5.48	0.013	0.055	0.11	-	0.002	V 0.97	23.5

*Nitride former based on thermodynamic data and/or phase diagrams

TABLE 2. APPLICABLE SPECIFICATIONS FOR THE SELECTED ALLOYS

Alloy	Hardware		Test Specimens	
	Form	Specifications	Form	Specifications
Haynes 188	Forging, bar	AMS 5772	Bar	AMS 5772
Rene'41	Forging	AMS 5713	Bar	AMS 5713
IN-100	--	--	Cast Bar	AMS 5397
Inconel 600	Forging, bar	MIL-N-6710	Bar	Hot-finished, pickled, and annealed

both of which are high in nitride formers; to compare three different Ni-base alloys showing a wide, uniform spread in content of nitride formers; and to compare cast versus wrought materials.

Haynes 188 will be used in the outer shell of the hydrazine-fueled, flight-type GG. The outer shell will be exposed to a $NH_3/N_2/H_2$ mixture at 1450 to 1650 F/700 psi. Under the present design and exposure conditions, low-cycle fatigue (LCF) is potentially the major failure mode. Therefore, LCF data are urgently needed for this set of conditions; the only available data were obtained in a hydrogen environment (Table 3).

The GG liner will be fabricated from Inconel 600 because of this material's excellent nitriding resistance. The liner has been designed to withstand temperatures from 1450 to 1850 F and an $NH_3/N_2/H_2$ pressure of 700 psi. Since this part will not be highly stressed, the possibility of a failure occurring is minimal.

Rene' 41 is the nozzle material in the two design versions of the fast-start turbine constructed within the past year under contract to the Air Force. The large heat flux and thermal cycling of the nozzle pose a potential LCF problem. This is the case also in the high-power turbine under study for the Air Force (Contract F33615-75-C-2072), where Rene' 41 is used for the nozzle and inlet manifold. Estimates of LCF life for Rene' 41 in a hydrogen environment are available (Table 3), but not in the nitriding environment that will be present in the fast-start turbine ($NH_3/N_2/H_2$ at 1450 to 1650 F/700 psi).

The IN-100 alloy was procured as vacuum cast bars. IN-100 was the only cast alloy to be studied. IN-100 has been successfully cast and used in a variety of shapes from turbine blades, vanes, and nozzles, to integral wheels. Isothermal forging processes, whereby disks are made out of powdered IN-100 at its superplasticity temperature, offer the potential that the alloy can be used as a wrought product.

TABLE 3. MINIMUM LOW-CYCLE FATIGUE PROPERTIES OF ALLOYS SELECTED FOR INVESTIGATION

Alloy	Temperature, F	Strain Range, percent	Approximate Cycles to Failure	Comments
Haynes 188	70	1.5	800	Wrought, H_2 Environment
	70	0.7	9000	
	1200	1.0	300	
	1200	0.5	8600	
	1500	1.5	60	
	1500	0.5	1200	
Inconel 600	-65 to 1850	1.5	200	Wrought, H_2 Environment; Estimated From Tensile Data
		0.5	600	
Rene' 41	-200 to 1600	1.3	110	Wrought, H_2 and H_2 Steam Environments; Estimated From Tensile Data
		0.6	4200	
IN-10C	70	1.5	100	As-Cast; Estimated From Tensile Data
	70	0.5	7500	
	1200	1.5	110	
	1200	0.5	37,000	
	1400	1.5	110	
	1400	0.5	37,040	
	1600	1.5	80	
	1600	0.5	14,310	

The available LCF and tensile data for the selected alloys at the initiation of the program, are presented in Tables 3 and 4, respectively. Unless specified otherwise, these are air values. The LCF data for Haynes 188 were obtained experimentally. For the other three alloys, they were predicted from tensile data using the Manson-Coffin equation.

TABLE 4. MINIMUM TENSILE PROPERTIES OF ALLOYS SELECTED FOR INVESTIGATION

Alloy	Yield Strength (YS), ksi				Ultimate Tensile Strength (UTS), ksi				% Reduction of Area (RA)				Comments
	70 F	1200 F	1400 F	1600 F	70 F	1200 F	1400 F	1600 F	70 F	1200 F	1400 F	1600 F	
Haynes 188	54	31	30	24	127	83	74	--	26	35	22	--	Wrought, Annealed, H_2/H_2O Environment (UTS, % RA), Air (YS)
Inconel 600	30	20	16	10	80	52	34	16	41	56	58	59	Wrought, Annealed
Rene' 41	130	119	109	75	170	148	126	87	10	18	8	16	Wrought, STA
IN-100	98	100	96	78	118	120	116	104	11	7	7	7	As-Cast

SPECIMEN DESIGN

The specimens for both the tension and low-cycle fatigue tests were hollow to permit internal pressurization with the gas mixture and thus obviate the need for a large external pressure vessel. The specimen design is shown in Fig. 1. For connection to the gas supply system, the Inconel 600 tubes shown are welded to the ends of the specimens.

It should be noted that the results of previous programs conducted at Rocketdyne have indicated that the low-cycle-fatigue life determined with hollow specimens is approximately one-half that determined with solid specimens. This difference does not affect the use of hollow specimens to determine environmental effects, but should be considered if the data are to be used for design purposes.

TEST CONDITIONS

In a hydrazine system gas generator, the hydrazine decomposes according to the equation:

$$N_2H_4 \rightarrow NH_3 + 1/2\ H_2 + 1/2\ N_2 \qquad (1)$$

This reaction is highly exothermic, resulting in gas temperatures above 2500 F. The ammonia formed by the decomposition of the hydrazine dissociates according to the equation:

$$NH_3 \rightarrow 1/2\ N_2 + 3/2\ H_2 \qquad (2)$$

This reaction is endothermic and, as the dissociation proceeds, the temperature drops. The relationship between temperature and percent NH_3 dissociation is shown in Fig. 2 (Ref. 15).

Ref. 15. Development of Design and Scaling Criteria for Monopropellant Hydrazine Reactors Employing Shell 405 Spontaneous Catalyst, Final Report on NASA Contract NAS-7-372, Rocket Research Corporation, Seattle, Washington, Report RRC-66-R-76, Vol. II, 18 January 1967.

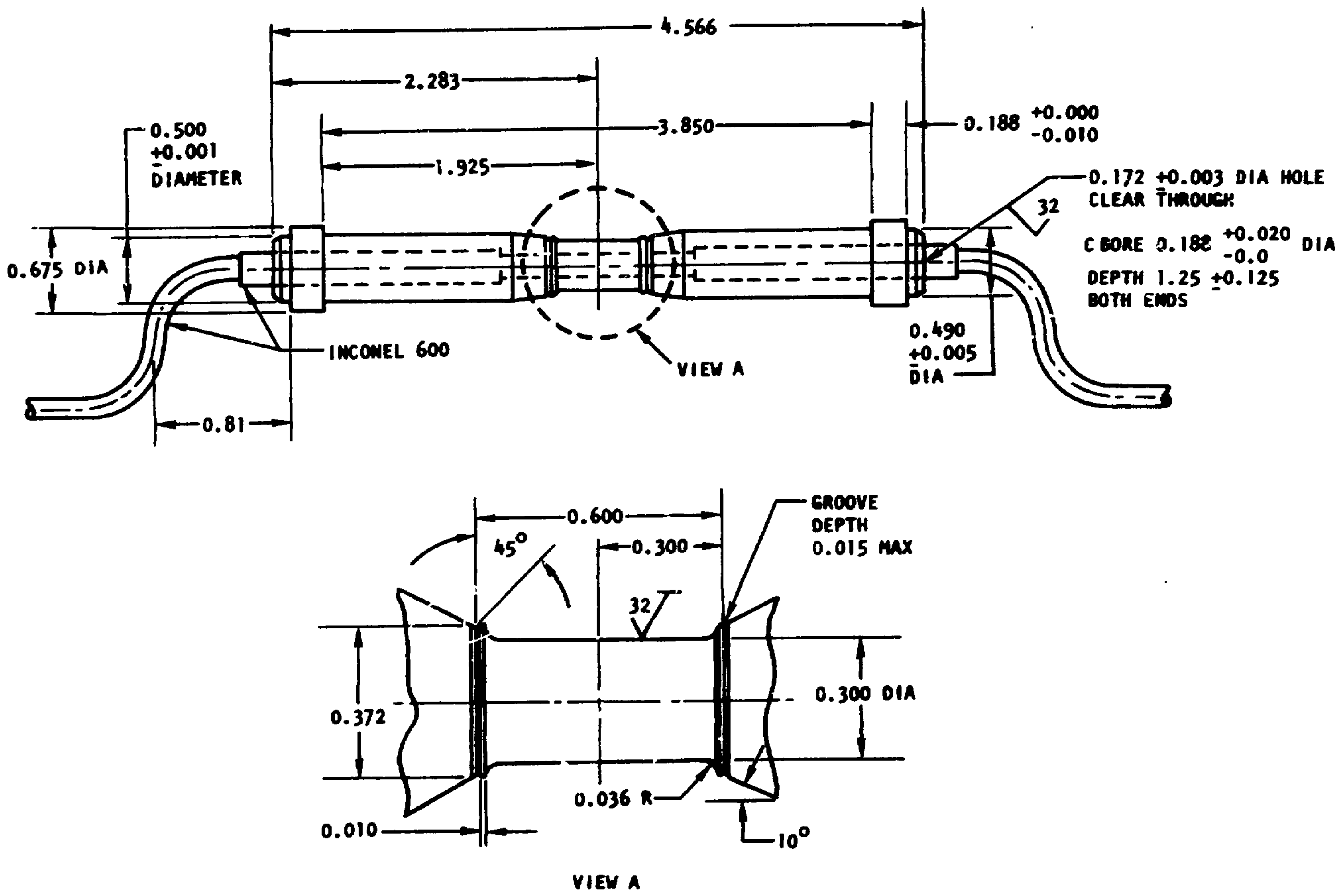

Figure 1. Test Specimen Design

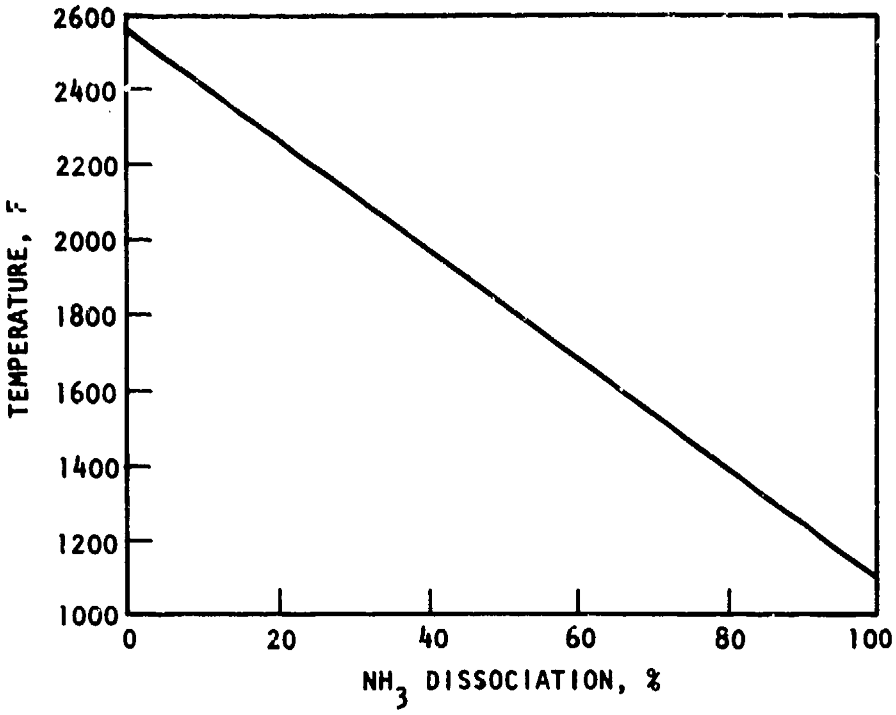

Figure 2. Relationship Between Temperature and Ammonia Dissociation in N_2H_4 Decomposition Products

Gas generator metal temperatures range from a high of approximately 1800 F down to approximately 1450 F. Turbine temperatures range from a high of approximately 1450 F down to 1250 F or possibly lower. To meet the objective of correlating test data with composition and microstructure for all the alloys, a base test temperature of 1450 F was selected as simulating reasonably well both gas generator and turbine temperatures. To assess the effect of temperature, a second test temperature of 1600 F, characteristic of higher gas generator temperatures, was selected for conducting a few tension tests on the gas generator materials - Haynes 188 and Inconel 600.

From Fig. 2, the degree of ammonia dissociation associated with the 1450 and 1600 F test temperature are 75 and 67%, respectively. Combining Eq. 1 and 2 for 75% ammonia dissociation, we have:

$$N_2H_4 \rightarrow 1/4\ NH_3 + 7/8\ N_2 + 13/8\ H_2 \qquad (3)$$

Equation 3 gives a gas composition (in mole %) of 9.1% NH_3, 31.8 N_2, and 59.1% H_2.

For 67% ammonia dissociation, we have:

$$N_2H_4 \rightarrow 1/3\ NH_3 + 5/6\ N_2 + 3/2\ H_2 \tag{4}$$

Equation 4 gives a gas composition (in mole %) of 12.5% NH_3, 31.25% N_2, and 56.25% H_2. Thus, these were the targeted test gas mixture compositions for the two temperatures. Figure 3 presents the relationship between the composition of hydrazine decomposition gas mixtures and the degree of ammonia dissociation.

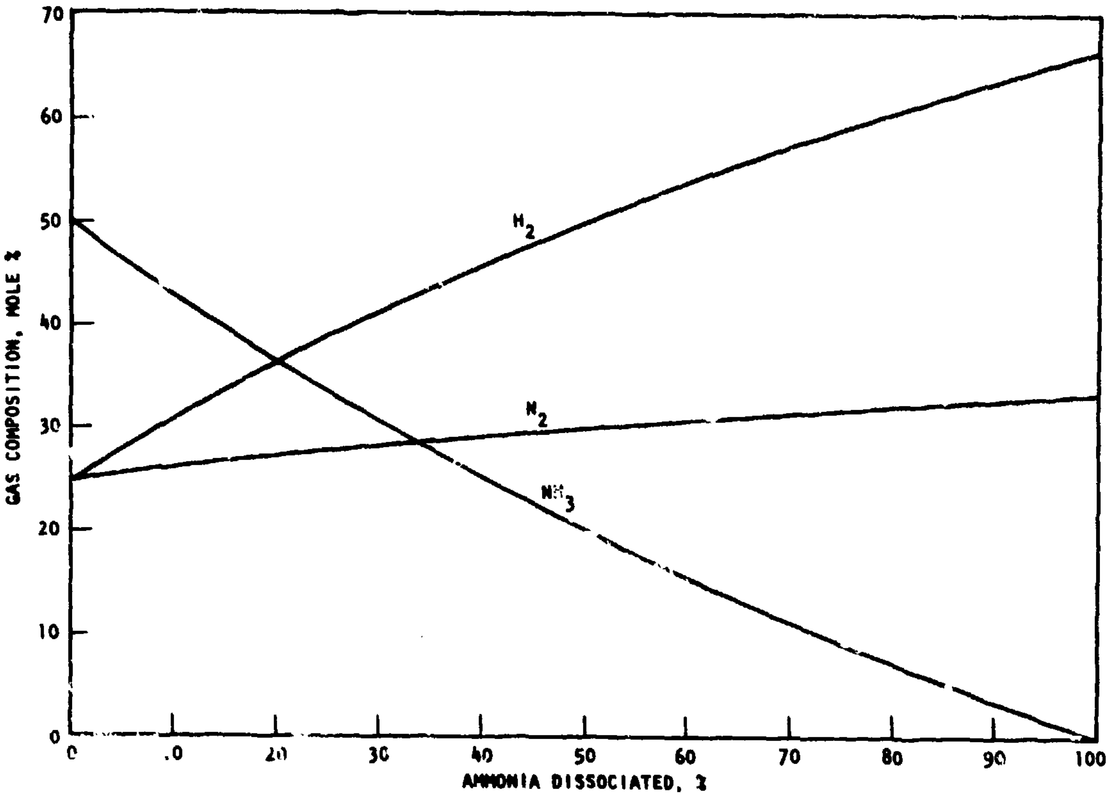

Figure 3. Relationship Between the Composition of Hydrazine Decomposition Gas Mixtures and the Degree of Ammonia Dissociation

Although direct analyses of gas samples from operating gas generators have not been conducted by Rocketdyne, indirect confirmation exists in the form of gas generator performance parameters, which indicate a molecular weight consistent with calculated gas compositions.

A gas mixture test pressure of 700 psi was selected as characteristic of APU gas pressures. A gas mixture flowrate through the specimen of approximately 0.5 lb/hr was used as being experimentally feasible while providing a flowrate rapid enough so that there would be no significant depletion of any gas component because of reaction with the metal. Assuming the 1450 F targeted gas mixture composition of 9.1% NH_3, 31.8% N_2, and 59.1% H_2, the calculated linear velocity associated with the 0.5 lb/hr flowrate is 2.6 ft/sec NH_3, 9.3 ft/sec N_2, and 17.2 ft/sec H_2 at standard temperature and pressure conditions, or 0.2 ft/sec NH_3, 0.7 ft/sec N_2, and 1.3 ft/sec H_2 at 1450 F and 700 psi.

GAS SUPPLY AND DISTRIBUTION SYSTEM

A schematic of the complex and unique gas supply and distribution system to supply the desired $NH_3/N_2/H_2$ gas mixtures under the appropriate conditions to the hollow test specimen is presented in Fig. 4, and a photograph of the system is shown in Fig. 5. Basically, the system consists of sources of high-pressure ammonia and nitrogen, with the NH_3 and N_2 metered into the system in proper proportion for the composition of N_2H_4, that is, according to the hypothetical equation:

$$3\ N_2H_4 \rightarrow 4\ NH_3 + N_2 \qquad (5)$$

Thus, the targeted metered-in gas composition (in mole %) is 80% NH_3 and 20% N_2.

The NH_3/N_2 gas mixture is passed through a preheater placed just before the test specimen to dissociate the ammonia to the required degree to give the required gas mixture composition. In this way, the gas species

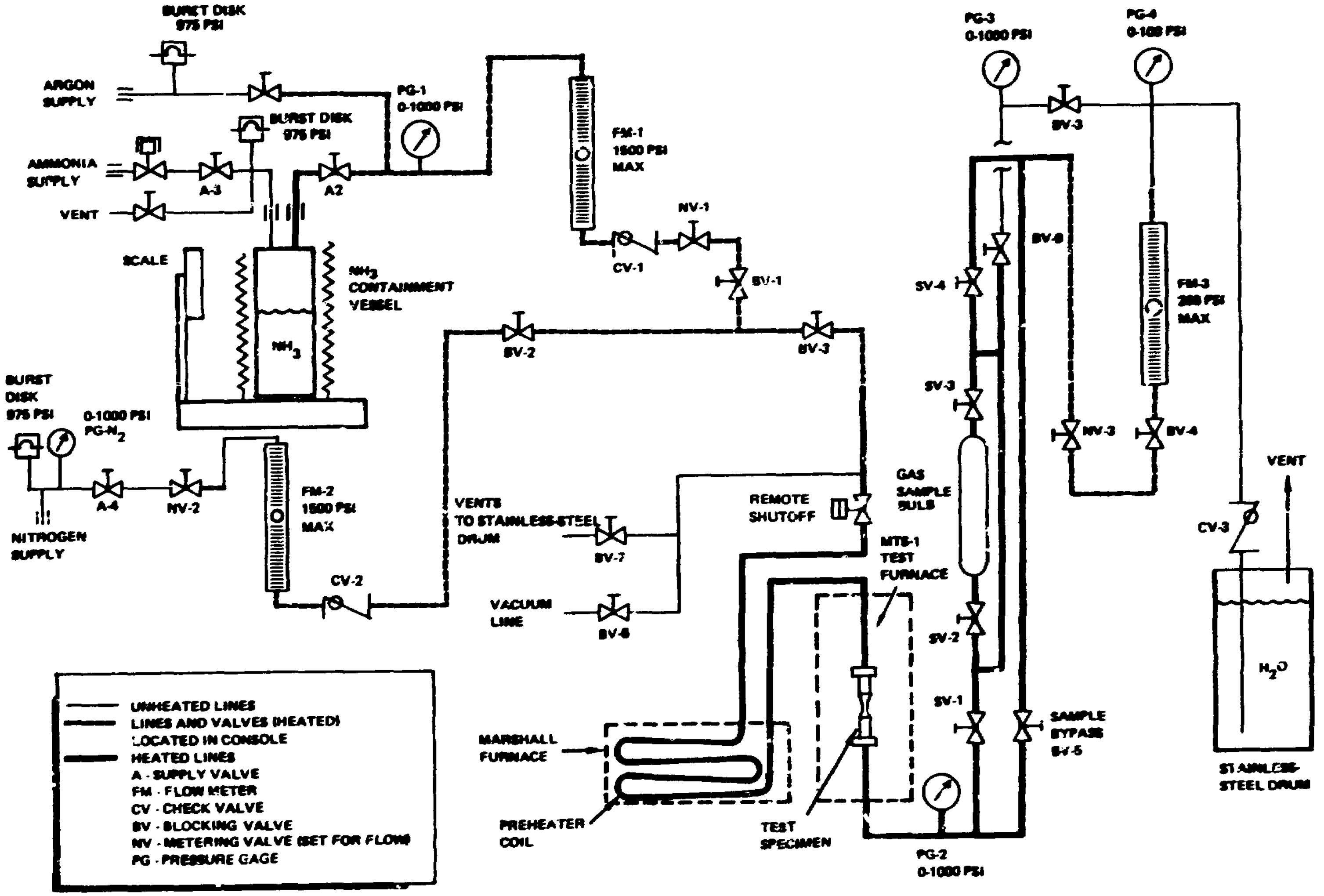

Figure 4 Schematic of Gas Supply and Distribution System

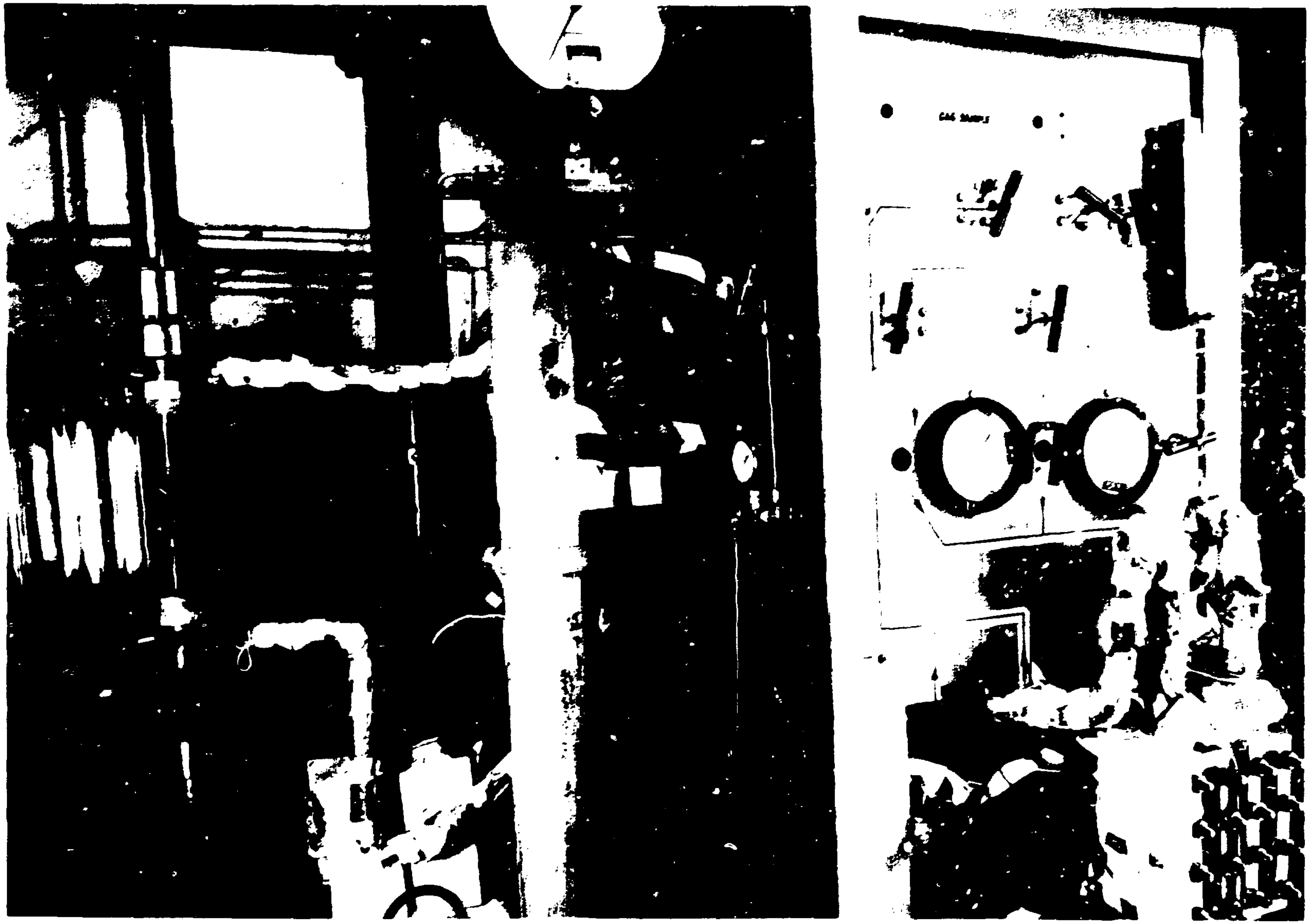

6DZ31-11/16/76-S1A

Figure 5. Gas Supply and Distribution System

flowing through the test specimen should simulate closely the gas flowing through a hydrazine system gas generator and turbine. The relationship between the composition of the test system gas mixtures and the degree of ammonia dissociation is given in Fig. 6.* Since a small amount of NH_3 dissociation also occurs in the test specimen, the gas sample for analysis is taken just downstream of the test specimen.

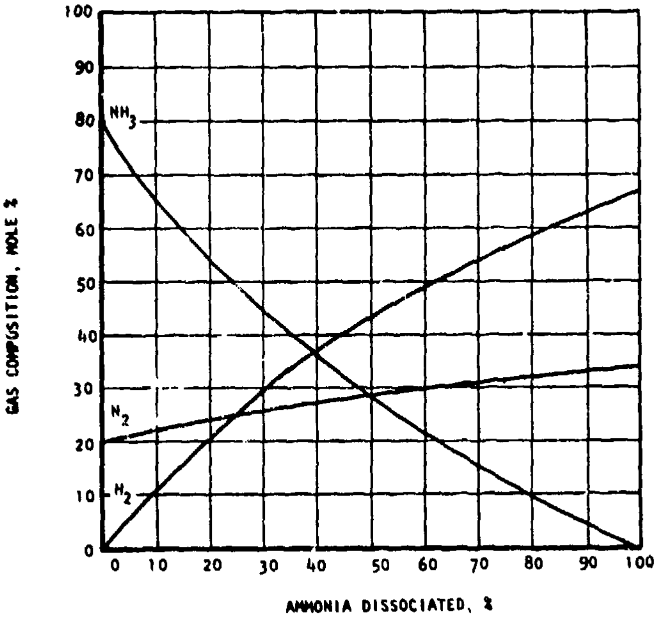

Figure 6. Relationship Between the Composition of Test System Gas Mixtures and the Degree of Ammonia Dissociation

The source of ammonia is a pressure vessel which is heated to the required temperature, approximately 190 F, to generate the necessary pressure (~780 psia) so that the pressure in the test specimen will be 700 psia. The relationship between ammonia pressure and temperature is shown in Fig. 7. All components of the system through which ammonia flows are heated by heating tapes to prevent condensation of the ammonia. The targeted temperature is 270 F, the critical temperature for ammonia.

---

*Figure 6 should not be confused with Fig. 3. Figure 3 relates gas composition with degree of ammonia dissociation in the $NH_3+\frac{1}{2}H_2+\frac{1}{2}N_2$ gas mixture resulting from the decomposition of hydrazine, while Fig. 6 relates gas composition with degree of ammonia dissociation in the $NH_3+\frac{1}{4}N_2$ gas mixture introduced into the test system.

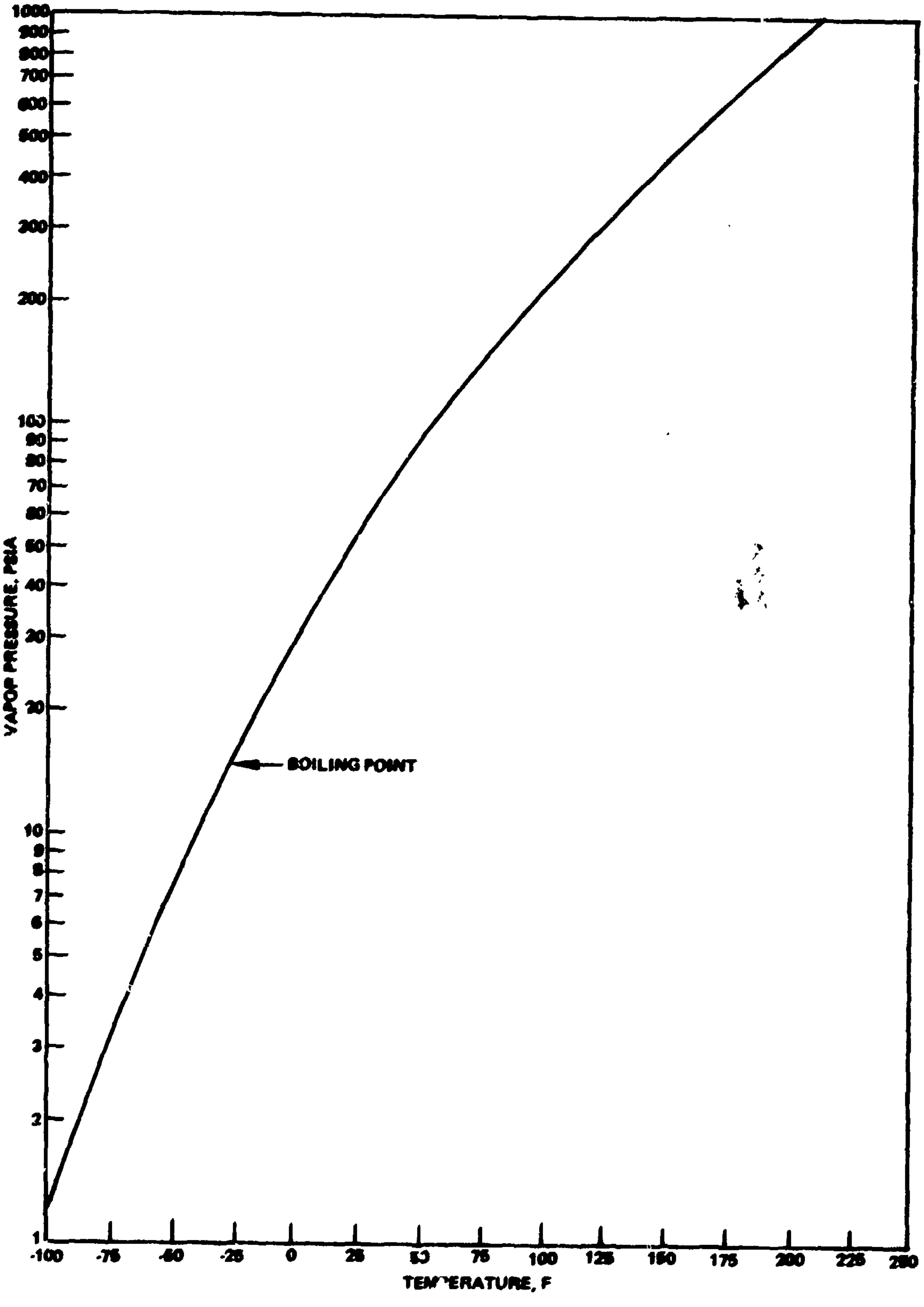

Figure 7. Relationship Between Ammonia Pressure and Temperature

During a test, the nitrogen pressure is regulated to be the same as the ammonia pressure. The metering valves NV-1 and NV-2 are used to control the flowrates of ammonia and nitrogen, respectively, to give the NH_3/N_2 mixture ratio of 4/1. The high-pressure, high-temperature flowmeters FM-1 and FM-2 used to measure the flowrates were not on hand at the initiation of the program. Thus, an attempt was made to operate only with the low-pressure flowmeter, FM-3, at the outlet of the system. In this case, it was necessary to independently regulate the ammonia flowrate then the nitrogen flowrate before combining the two gases. After a number of attempts, this procedure was abandoned because of inability to maintain NH_3/N_2 ratios. Also, the degree of dissociation of the ammonia is not only a function of the temperature of the preheater coil, but also the dwell time and, therefore, the ammonia flowrate in the coil. Thus, without active control of the ammonia flowrate, the degree of ammonia dissociation was erratic. Proper flowmeters eliminated this problem.

The first attempt to use the high-pressure, elevated-temperature flowmeters resulted in serious leakage in the ammonia flowmeter. It was found that even though the time of exposure to ammonia was short, gaskets and O-ring seals were badly deteriorated and cracked. Although the flowmeters were purchased specifically for ammonia service, it was established that the vendor had used Viton A for the gaskets and O-rings, a material not compatible with ammonia under the exposure conditions. The ammonia flowmeter was outfitted with neoprene gaskets and O-rings, and no further problems were experienced.

A change also was made in the gas sampling system. In the initial system, a gas sample was taken by means of a sample bulb attached to the flowing gas system. Because of the relatively large volume of the sample bulb, a pressure drop occurred, and this affected the NH_3/N_2 ratio. With the current system (shown in Fig. 4), gas flow is established through the sample bulb line and a parallel line. When a sample is taken, the sample bulb is simply closed off, with no change in pressure in the system.

During checkout of the system, leaks occurred in various parts exposed to ammonia. Basically, the problem was that the initial system was constructured with AN (Air Force-Navy Aeronautical Standards) fittings which had the required pressure capability and were considered suitable for the application. However, sealing materials were not adequately compatible with ammonia, and the fittings did not remain pressure-tight through the temperature cycling. The ammonia system was completely reworked with high-pressure fittings (Autoclave Engineering Co.) which utilize metal-to-metal seals, which solved the leakage problems.

TEST PROCEDURE

In accordance with the earlier discussions, the tension tests were performed using specimens internally pressurized to 700 psi by the flowing $NH_3/N_2/H_2$ gas mixture with composition appropriate to the temperature, or by flowing argon to establish a baseline for determining environmental effects. To separate time-dependent from time-independent environmental effects, tests were conducted for all four materials at 1450 F after zero exposure and after a 2-hour exposure to the $NH_3/N_2/H_2$ gas mixture prior to tension testing. The 1600 F tension tests on Haynes 188 and Inconel 600 were conducted after a 2-hour exposure to the $NH_3/N_2/H_2$ gas mixture.

The low-cycle fatigue tests were performed at 1450 F, with the specimens internally pressurized to 700 psi by the $NH_3/N_2/H_2$ gas mixture or by flowing argon. The low-cycle fatigue tests were strain-cycling tests with a sawtooth, compressive cycle (zero to maximum compressive strain) at a frequency of 0.5 Hz. This cycle simulates the thermal strain cycle experienced by the hydrazine APU components. The frequency was selected as being slow enough to allow for the effect on cyclic life of any time-dependent damage mechanisms, such as accumulated plastic strain, creep strain, and environmental interactions. The tests were conducted at two strain ranges, usually at approximately 1.5 and 0.8%. A few tests were conducted with longer time cycles to determine the effect of cyclic frequency on low-cycle fatigue life. These tests were performed at a frequency of 0.1 Hz using a square wave form with a 0.5-second ramp to the maximum compressive strain, a 9-second hold period at the maximum strain, and a 0.5-second ramp from maximum strain to zero. All of these tests were performed with a strain range of 1%.

Both tension tests and low-cycle fatigue tests were performed with an electrohydraulic, closed-loop (MTS) machine shown in Fig. 5. The specimens were heated by a quartz lamp furnace (Fig. 5) with argon flowing around and through the specimen. Heat-up time was approximately 30 minutes. When the test was to be an argon test, it was initiated as soon as the test temperature was attained. When the test was to be one with the $NH_3/N_2/H_2$ gas mixture, the gas flowing through the specimen was switched to that gas when the test temperature was attained. This resulted in a temperature drop of approximately 40 F, and stabilization of the test temperature and gas flow required approximately 30 minutes before the test could be initiated. Thus, even for so-called "zero-hold time", $NH_3/N_2/H_2$ test specimens were at temperatures approaching the test temperature for some 30 minutes before testing. For all tests, an argon flow through the furnace and around the specimen was maintained throughout the test. The $NH_3/N_2/H_2$ gas samples for analysis were taken when test parameters had been stabilized and just prior to the initiation of the tension or low-cycle fatigue test. $NH_3/N_2/H_2$ gas samples were not taken before every test, but sufficient samples were taken to ensure that the system was operating properly to give gas compositions adequately simulating those from hydrazine gas generators.

RESULTS AND DISCUSSION

TENSION TESTS

The results of the tension tests are presented in Table 5 . In no case is there any significant effect on tensile properties attributable to the $NH_3/N_2/H_2$ environments. For Haynes 188, the small decrease in yield strength and increase in ductility of the specimens tested with $NH_3/N_2/H_2$ compared to those tested with argon may be attributable to the longer time at temperature. As noted earlier, even the "zero-hold time," $NH_3/N_2/H_2$ test specimens were at temperatures approaching the test temperature for some 30 minutes to stabilize test parameters before initiating a tension test, while the argon tension tests were initiated as soon as the specimen attained the test temperature. The only significant differences in tensile properties among the Inconel 600 specimens were the lower strengths and higher reductions in area at 1600 F (attributable to the higher temperature). For Rene' 41, the slightly higher strength and lower ductility of specimens tested with $NH_3/N_2/H_2$ compared to those tested with argon are not believed to be significant. The results for IN-100 were erratic because of microporosity in the cast bars and the intrinsic low ductility of that alloy.

METALLOGRAPHY OF TENSILE SPECIMENS

Selected tension-tested specimens were examined by optical microscopy to determine if any nitriding had occurred with the $NH_3/N_2/H_2$ environments or if any other structural differences resulted from the exposure to those environments as compared to argon. The specimens examined had been tested at 1450 F with argon or with the $NH_3/N_2/H_2$ environment after a 2-hour exposure to that environment. No nitriding or other structural effects of the $NH_3/N_2/H_2$ environments on any of the materials were apparent from the metallographic examination.

TABLE 5. TENSILE PROPERTIES OF FOUR ALLOYS EXPOSED TO 700-PSI ARGON AND $NH_3/N_2/H_2$ ENVIRONMENTS

Material	Specimen Number	Environment (numbers are mole %) NH_3	N_2	H_2	Test Temperature, F	Hold Time Prior to Tension Test, hours*	Yield Strength, ksi	Ultimate Tensile Strength, ksi	Reduction of Area, %	Elongation, %
Haynes 188	1		Argon		1450	0	40.1	88.5	25.4	24.7
	2		Argon		1450	0	40.4	85.2	20.1	22.8
	3a	4.2	42.1	53.7	1450	0	37.2	84.9	33.9	28.3
	7	11.1	29.0	59.9	1450	2	35.5	83.8	37.5	36.5
	11	11.1	29.0	59.9	1450	2	36.9	85.8	37.2	41.3
	12	20.3	27.5	52.2	1600	2	36.1	78.5	42.6	33.2
	15	11.6	29.9	58.8	1600	2	35.5	70.9	51.5	39.4
Inconel 600	1		Argon		1450	0	26.9	48.1	64.7	45.7
	2		Argon		1450	0	30.1	47.5	65.3	54.5
	3	10.9	37.8	51.3	1450	0	26.7	47.4	61.9	50.4
	6	11.1	29.0	59.9	1450	2	23.9	46.3	58.3	39.8
	7	11.1	29.0	59.9	1450	2	25.1	45.6	62.5	50.7
	12	20.3	27.5	52.2	1600	2	17.7	34.4	86.1	39.7
	16	11.6	29.9	58.5	1600	2	16.4	29.5	86.3	47.6
Rene' 41	1		Argon		1450	0	113.2	160.6	21.3	21.3
	2		Argon		1450	0	112.4	165.2	23.0	21.9
	3	5.0	32.3	62.7	1450	0	129.7	175.7	20.7	15.7
	9	11.1	29.0	59.9	1450	2	123.2	172.3	18.9	17.0
	13	11.1	29.0	59.9	1450	2	121.6	164.6	20.0	14.0
IN-100	13		Argon		1450	0	112.8	133.9	10.7	8.2
	16		Argon		1450	0	115.3	115.7	1.8	5.2
	3	8.5	27.0	64.5	1450	0	118.4	118.4	2.0	3.6
	10	11.1	29.0	59.9	1450	2	112.0	126.3	10.0	5.0
	14	11.1	29.0	59.9	1450	2	121.6	122.9	5.8	3.8

*NOTE: All $NH_3/N_2/H_2$ specimens exposed approximately 30 minutes at temperatures approaching test temperature before tensile test or hold time initiated

LOW-CYCLE FATIGUE TESTS

The results of the low-cycle fatigue tests with the 0.5 Hz frequency are presented in Tables 6 through 9 and Fig. 8 through 15. There is no uniquely defined or universally accepted criterion for failure in low-cycle fatigue tests. Simple specimen separation may be misleading as a failure criterion. For example, in this program, some specimens developed multiple through-the-wall cracks, and the specimens were acting like a hinge or double hinge during cycling. In such a case, the specimen may withstand a very large number of cycles before final separation. Thus, for this program, the low-cycle fatigue data were analyzed to determine the number of cycles to a 5% and a 40% load decrease, and these were used to evaluate the effect of the $NH_3/N_2/H_2$ environments. It is believed that in most cases crack initiation had occurred by the time the load had decreased 5%, and that a crack had grown through the wall by the time the load had decreased 40%. A number of specimens were intentionally not cycled to complete separation, so that the fracture surfaces could be retained in an undamaged state. These specimens were tension tested to failure at the test temperature (1450 F), and the residual tensile strength is recorded in Tables 6 through 9.

A perusal of Tables 6 through 9 and Fig. 8 through 15 reveals the following. The low-cycle-fatigue life of Haynes 188 was somewhat lower with $NH_3/N_2/H_2$ environments than with argon. The reduction was slightly larger at the higher strain ranges than at the lower. The effect was essentially the same for the 5% and the 40% load decrease criteria. The low-cycle-fatigue life of Inconel 600 was somewhat lower with $NH_3/N_2/H_2$ environments than with argon at the higher strain range. There was no apparent effect of the $NH_3/N_2/H_2$ environments on the low-cycle-fatigue life of Inconel 600 at the lower strain range, but the results are ambiguous because of the wide scatter of the results for the argon tests. There was no apparent effect of the $NH_3/N_2/H_2$ environments on the low-cycle-fatigue life of either Rene' 41 or IN-100. The low-cycle-fatigue results were more erratic for IN-100 than for the other metals, probably

TABLE 6. LOW-CYCLE FATIGUE PROPERTIES OF HAYNES 188 EXPOSED TO 700-PSI ARGON AND $NH_3/N_2/H_2$ AT 1450 F

Environment (numbers are mole %)			Specimen Number	Strain			Number of Cycles			Load Decrease at End of Cycling, %	Location of Failure	Comments
NH_3	N_2	H_2		Maximum, %	Minimum, %	Range, %	5% Load Decrease	40% Load Decrease	Total Number of Cycles			
	Argon		9	1.46	0.02	1.44	157	167	220	100	Top radius	No other cracks
	Argon		6	1.57	0.00	1.57	86	93	115	83	Both radii	No other cracks Tensile: 1120 pounds
	Argon		4	0.82	0.08	0.74	579	600	742	77	Bottom radius	No other cracks Tensile: 920 pounds
	Argon		14	0.80	0.00	0.80	622	644	902	75	Top radius	ID bore marks Tensile: 2000 pounds
7.5	34.0	58.5	13	1.50	0.17	1.33	72	78	102	100	Both radii	Some other cracks inside and out
4.4	33.9	61.7	10	1.50	0.02	1.48	69	74	103	100	Bottom radius	No other cracks
12.0	33.0	55.0	5	0.80	0.00	0.80	325	383	635	100	Top radius	No other cracks
6.1	30.5	63.4	8	0.80	0.02	0.78	516	548	715	78	Bottom radius	ID bore marks; no cracks Tensile: 350 pounds

TABLE 7. LOW-CYCLE FATIGUE PROPERTIES OF INCONEL 600 EXPOSED TO 700-PSI ARGON AND $NH_3/N_2/H_2$ AT 1450 F

Environment (numbers are mole %)			Specimen Number	Strain			Number of Cycles			Load Decrease at End of Cycling, %	Location of Failure	Comments
NH_3	N_2	H_2		Maximum, %	Minimum, %	Range, %	5% Load Decrease	40% Load Decrease	Total Number of Cycles			
Argon			9	1.46	0.08	1.38	403	442	499	100	Top radius	Center bulge
Argon			8	1.52	0.02	1.50	252	286	330	100	Both radii	Center bulge Tensile: 980 pounds
Argon			4	0.82	0.00	0.82	824	922	962	100	Top radius	Cracks - bottom radius Center bulge
Argon			14	0.80	0.02	0.78	408	462	602	65	Both radii	Center bulge Tensile: 1070 pounds
8.0	31.0	61.0	13	1.48	0.02	1.46	141	154	182	100	Both radii	Center bulge
4.4	33.9	61.7	10	1.50	0.02	1.48	232	253	275	100	Top radius	Center bulge
12.0	30.0	58.0	5	0.80	0.02	0.78	680	875	1221	85	Both radii and 1 inch from bottom	Cracks 10, bulge Tensile: 930 pounds
8.8	31.8	59.4	15	0.82	0.02	0.80	582	672	751	60	Both radii	Center bulge Tensile: 1560 pounds

TABLE 8. LOW-CYCLE FATIGUE PROPERTIES OF RENE' 41 EXPOSED TO 700-PSI ARGON AND $NH_3/N_2/H_2$ AT 1450 F

Environment (numbers are mole %)			Specimen Number	Strain			Number of Cycles			Load Decrease at End of Cycling, %	Location of Failure	Comments
NH_3	N_2	H_2		Maximum, %	Minimum, %	Range, %	5% Load Decrease	40% Load Decrease	Total Number of Cycles			
	Argon		9	1.50	0.60	0.90	854	876	888	100	Bottom radius	No other cracks
	Argon		4	1.52	0.05	1.47	24	215	221	100	Top radius	No other cracks
	Argon		16	0.80	0.08	0.72	1371	1913	2014	71	Bottom radius	Cracks - top radius Tensile: 1840 pounds
	Argon		8	0.80	0.05	0.75	1904	2170	2235	69	Bottom radius	Some small ID cracks Tensile: 2000 pounds
8.0	31.0	61.0	11	1.53	0.37	1.16	140*	142	142	100	Top radius	Some other cracks inside and out
4.4	33.9	61.7	6	1.52	0.02	1.50	44	288	288	100	Bottom radius	No other cracks
12.0	30.0	58.0	5	0.80	0.03	0.77	1033	1954	2024	100	Top radius	No other cracks
6.1	30.5	63.4	12	0.82	0.02	0.80	1568	2320	2401	70	Bottom radius	ID bore marks Tensile: 2040 pounds

*Preceeded by 50 cycles with 1.1% maximum strain, 0.32% minimum strain

TABLE 9. LOW-CYCLE FATIGUE PROPERTIES OF IN-100 EXPOSED TO 700-PSI ARGON AND $NH_3/N_2/H_2$ AT 1450 F

Environment (numbers are in mole %)			Specimen Number	Strain			Number of Cycles			Load Decrease at End of Cycling, %	Location of Failure	Comments
NH_3	N_2	H_2		Maximum, %	Minimum, %	Range, %	5% Load Decrease	40% Load Decrease	Total Number of Cycles			
	Argon		9	1.50	0.40	1.10	123	126	126	100	Straight section	Some other cracks inside and out
	Argon		7	1.53	0.00	1.53	1	1	1	100	Straight section	Inclusion in fracture Cracks, ID
	Argon		12	1.46	0.02	1.44	3	3	3	100	Straight section	Crack, ID radius
	Argon		8	1.10	0.50	0.60	540	*			Straight section	Hole off center
	Argon		4	0.80	0.08	0.74	525	979	1501	83	Both radii and straight section	No other cracks Tensile: 920 pounds
8.0	31.0	61.0	1	1.53	0.67	0.96	79	80	80	100	Straight section	Some other cracks; most inside
14.0	31.5	54.5	15	1.46	0.03	1.43	3	5	5	100	Straight section	No other cracks
12.0	30.0	58.0	6	0.80	0.08	0.72	137	829	1145	100	Top radius	No other cracks
6.1	30.5	63.4	11	0.80	0.10	0.70	1099	2301	2801	76	Bottom radius	No other cracks Tensile: 1060 pounds

*Strain range increased at 575 cycles

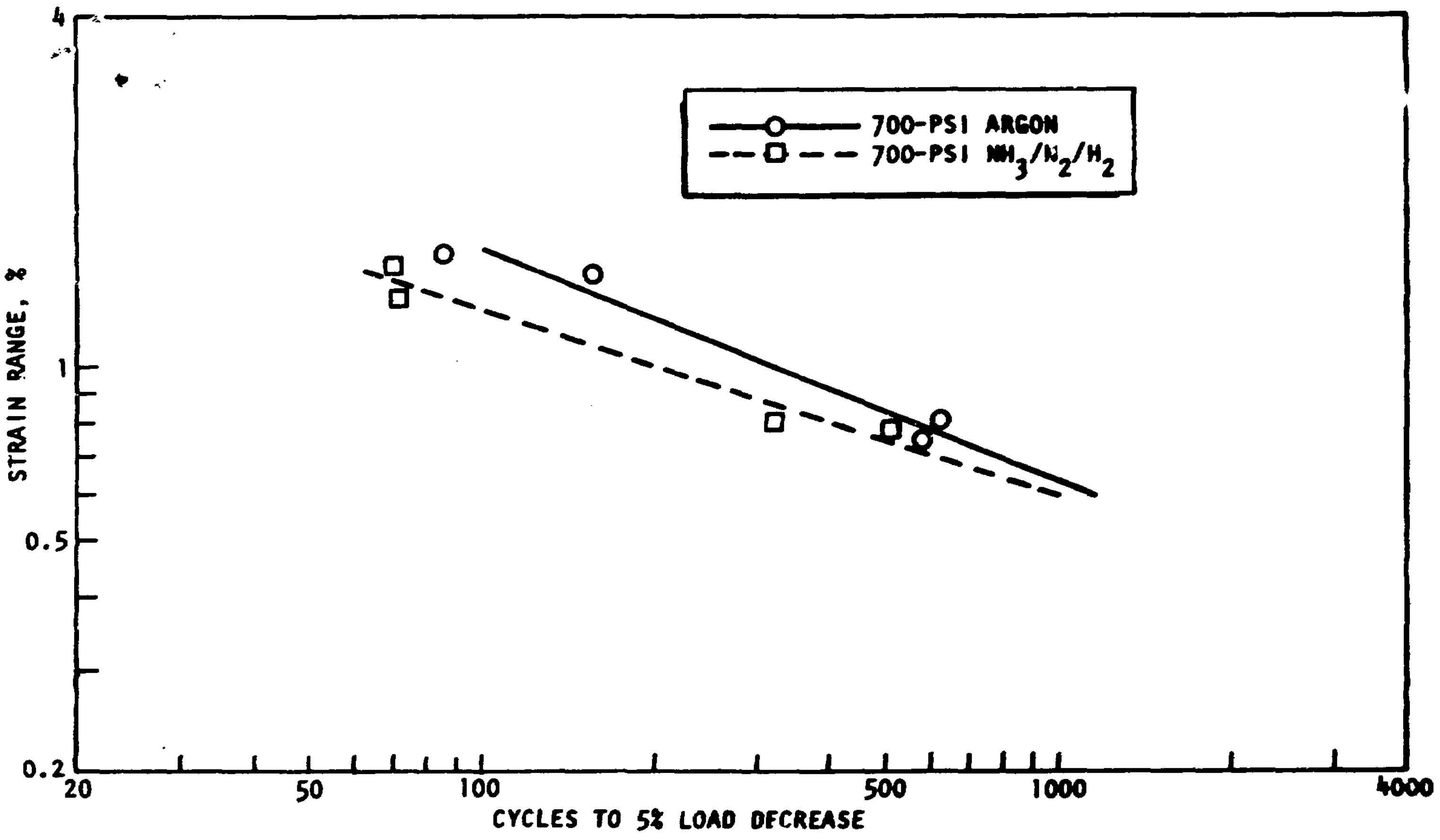

Figure 8. Number of Cycles to 5% Load Decrease vs Strain Range for Haynes 188 at 1450 F

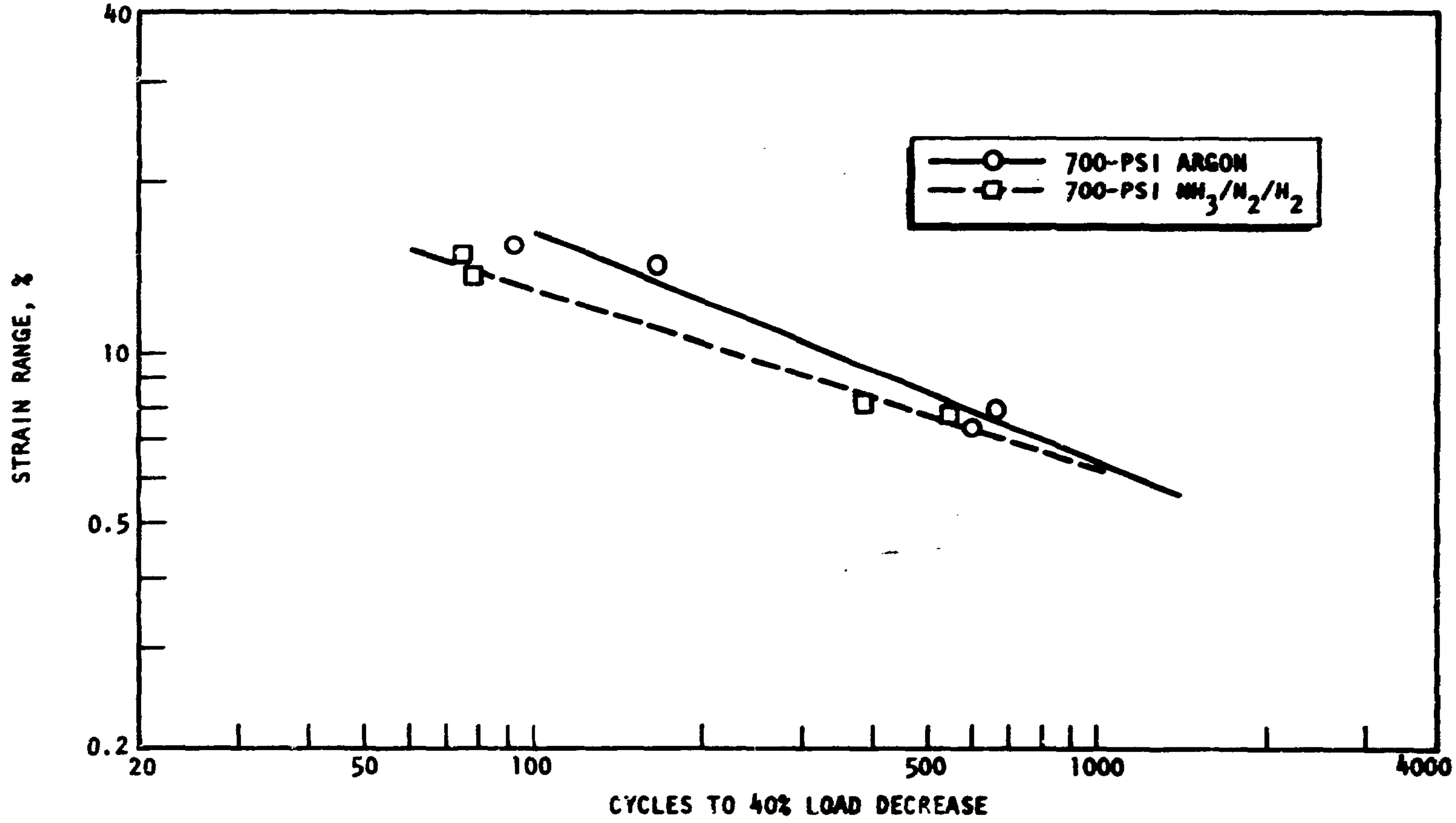

Figure 9. Number of Cycles to 40% Load Decrease vs Strain Range for Haynes 188 at 1450 F

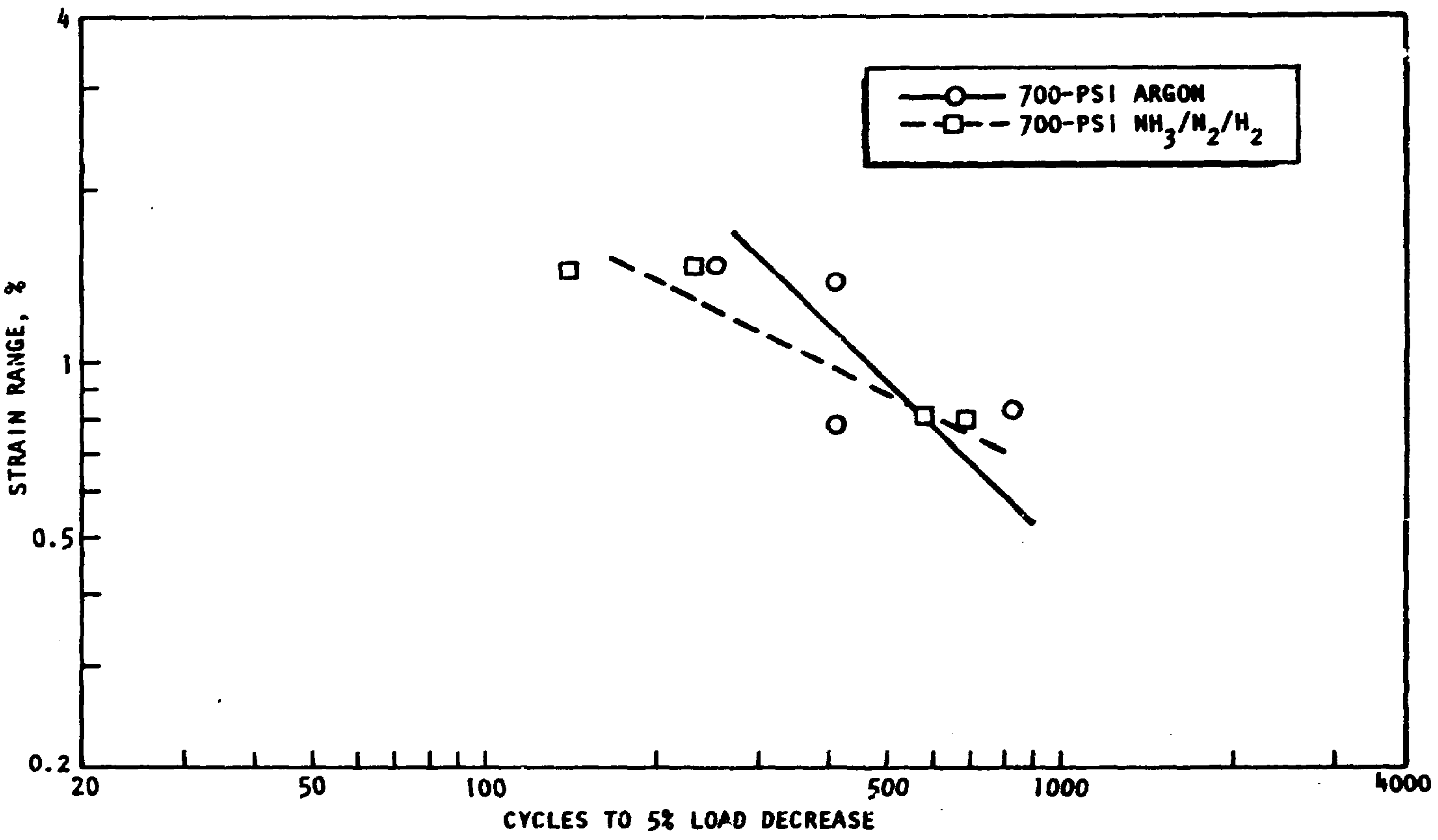

Figure 10. Number of Cycles to 5% Load Decrease vs Strain Range for Inconel 600 at 1450 F

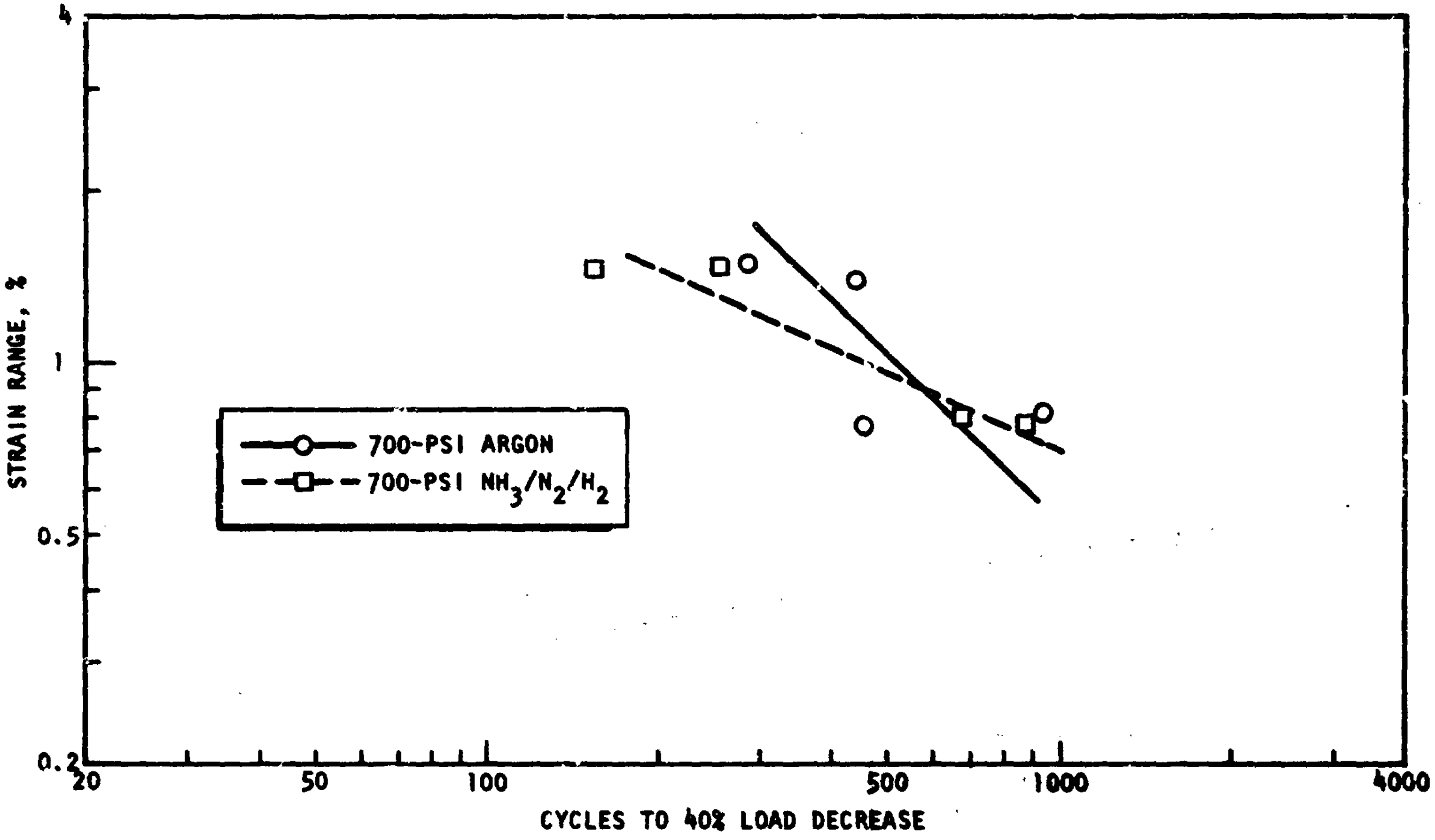

Figure 11. Number of Cycles to 40% Load Decrease vs Strain Range for Inconel 600 at 1450 F

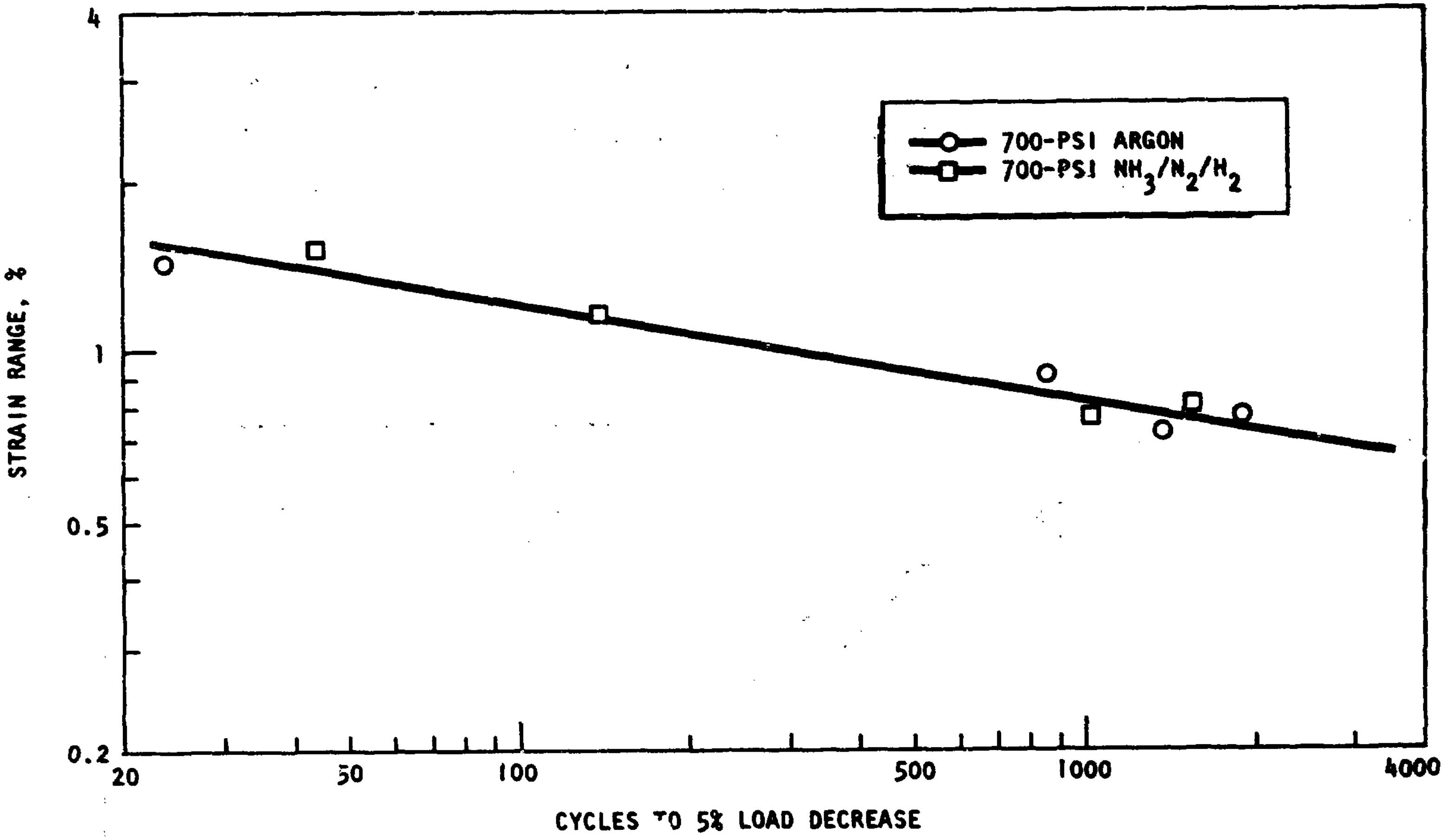

Figure 12. Number of Cycles to 5% Load Decrease vs Strain Range for Rene' 41 at 1450 F

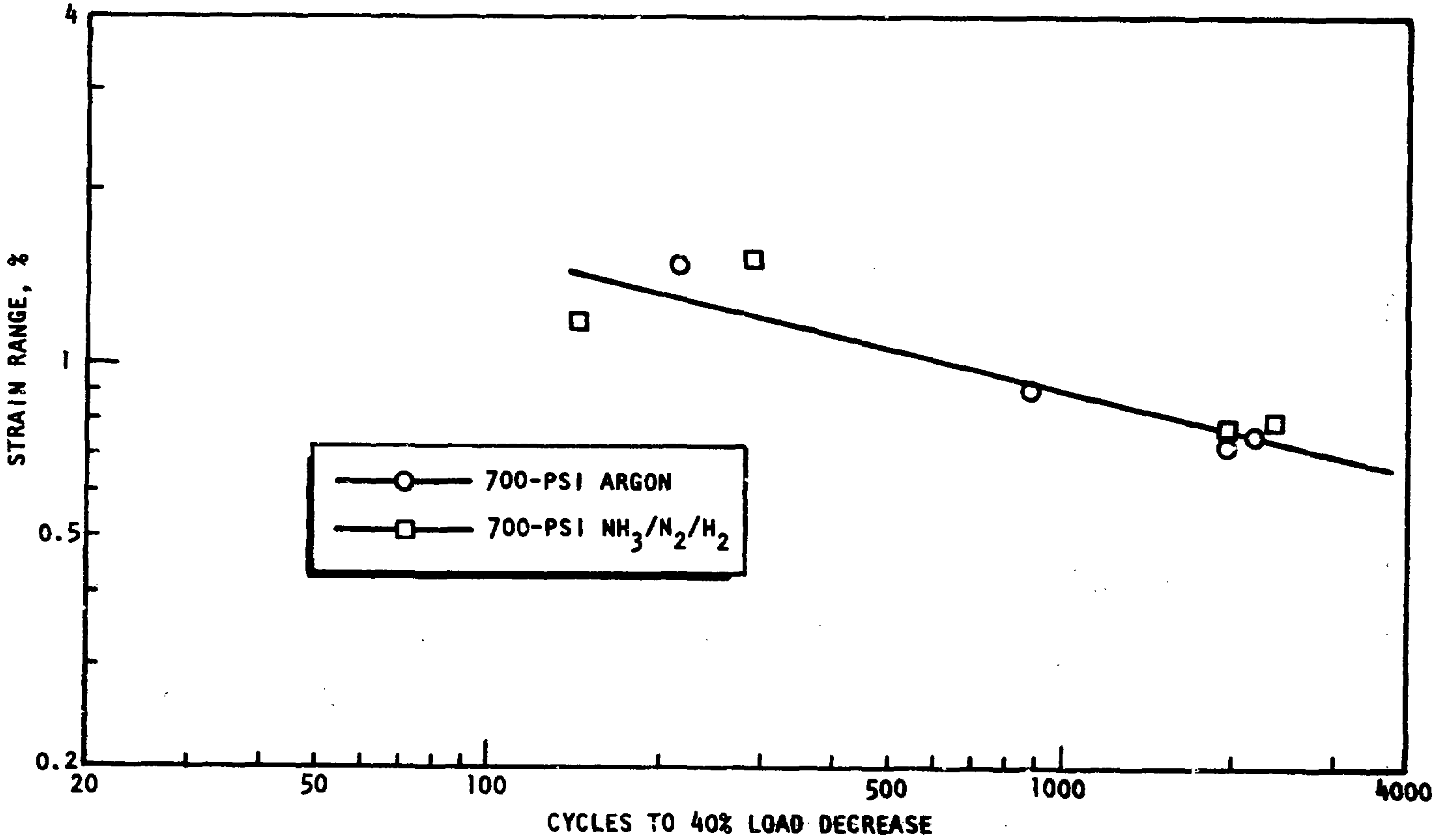

Figure 13. Number of Cycles to 40% Load Decrease vs Strain Range for Rene' 41 at 1450 F

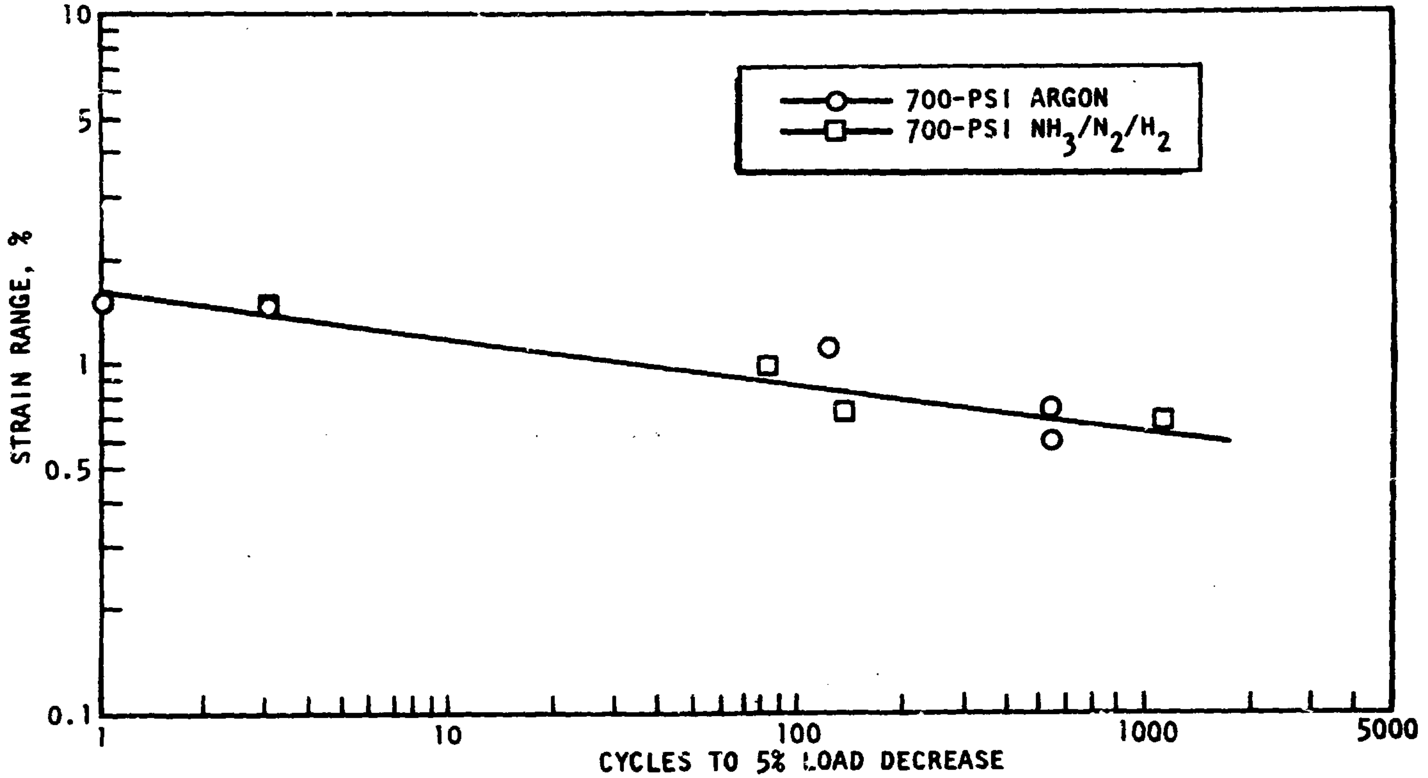

Figure 14. Number of Cycles to 5% Load Decrease vs Strain Range for IN-100 at 1450 F

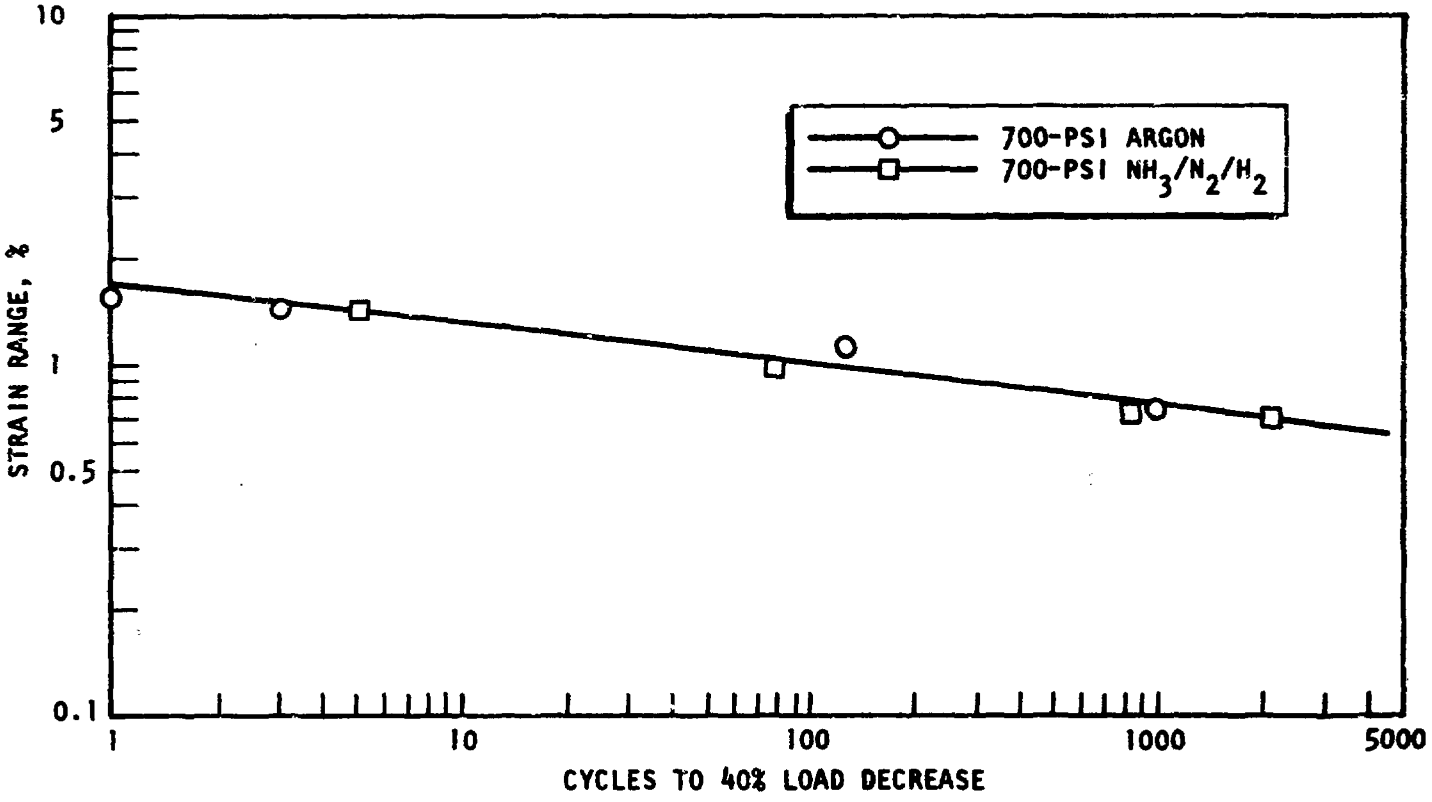

Figure 15. Number of Cycles to 40% Load Decrease *vs* Strain Range for IN-100 at 1450 F

because of porosity and inherent low ductility of the cast specimen bars. The low-cycle-fatigue specimens of Haynes 188, Inconel 600, and Rene' 41 all failed in the radii at the ends of the straight gage section because of the small stress concentration at that location. Most of the IN-100 specimens failed in the straight section. The IN-100 specimens were sufficiently brittle that a strain range of 1.5%, or near 1.5%, led to failure in the first or very few cycles.

As noted earlier, a limited number of longer-cycle, 0.1 Hz frequency tests were conducted to determine the effect of cyclic frequency on low-cycle fatigue life. Tests were performed with Haynes 188, Inconel 600, and Rene' 41 specimens at 1450 F with a strain range of 1%, and the results are presented in Table 10. Table 11 presents a comparison between the 0.1 Hz and 0.5 Hz frequency tests in terms of the number of cycles to a designated load decrease. Data for the 0.5 Hz frequency conditions were obtained from the curves in Fig. 8 through 13.

It can be seen from Table 11 that in all cases the longer cycle significantly reduced the low-cycle fatigue life for both argon and $NH_3/N_2/H_2$ environments and the percentage reduction was greater for $NH_3/N_2/H_2$ environments, particularly for Haynes 188 and Inconel 600 alloys. In the case of Rene 41, the effect of the $NH_3/N_2/H_2$ environment was less pronounced, although measureably lower life was noted in that environment in terms of the number of cycles to 40% load drop.

ELECTRON FRACTOGRAPHY OF LOW-CYCLE-FATIGUE TESTS

Selected low-cycle-fatigue specimens were examined by scanning electron microscopy in a search for any differences in the fracture appearance between specimens exposed to argon and those exposed to $NH_3/N_2/H_2$ environments. Since the greatest evidence of $NH_3/N_2/H_2$ effects on low-cycle-fatigue life occurred at the higher strain ranges, such specimens were selected for electron fractography. The specimens were chosen so that the argon and $NH_3/N_2/H_2$ exposures had been tested at strain ranges as close as possible to each other.

TABLE 10. LOW-CYCLE FATIGUE PROPERTIES OF MATERIALS IN 700-PSI ARGON AND $NH_3/N_2/H_2$ AT 1450 F (Hz = 0.1)

Material	Environment (numbers are mole %)			Specimen Number	Strain			Number of Cycles			Load Decrease at end of Cycling %	Location of Failure	Comments
	NH_3	N_2	H_2		Maximum %	Minimum %	Range %	5% Load Decrease	40% Load Decrease	Total Number of Cycles			
Haynes 188	Argon			17	1.0	0	1.0	212	232	237	62	Bottom Radius	Center bulge Tensile: 1390 pounds
	5.1	31.8	63.1	16	1.0	0	1.0	81	98	110	58	Bottom Radius	Center bulge Tensile: 1600 pounds
Inconel 600	5.1	31.8	63.1	17	1.0	0	1.0	178	178	178	100	Top Radius	Center bulge Cracks - bottom radius
Rene' 41	Argon			15	1.0	0	1.0	26	580	597	64	Top Radius	Cracks - bottom radius Tensile: 2130 pounds
	4.6	28.8	66.6	14	1.0	0	1.0	31	440	442	48	Top Radius	Cracks - bottom radius Tensile: 2130 pounds

TABLE 11. EFFECT OF CYCLIC FREQUENCY ON LOW-CYCLE FATIGUE LIFE OF ALLOYS EXPOSED TO ARGON AND $NH_3/N_2/H_2$ ENVIRONMENTS AT 1450 F (Strain Range = 1%)

Material	Load Decrease, %	Environment	Number of Cycles to Designated Load Decrease		$N_{0.1\ Hz}/N_{0.5\ Hz}$	
			Hz = 0.5 (From Fig. 8 through 13)	Hz = 0.1	A	$NH_3/N_2/H_2$
Haynes 188	5	A	315	212	0.67	
	5	$NH_3/N_2/H_2$	200	81		0.41
	40	A	335	232	0.69	
	40	$NH_3/N_2/H_2$	225	98		0.44
Inconel 600	5	A	463			
	5	$NH_3/N_2/H_2$	385	178		0.46
	40	A	510			
	40	$NH_3/N_2/H_2$	460	178		0.39
Rene' 41	5	A	300	26	0.09	
	5	$NH_3/N_2/H_2$	300	31		0.10
	40	A	630	580	0.92	
	40	$NH_3/N_2/H_2$	630	440		0.70

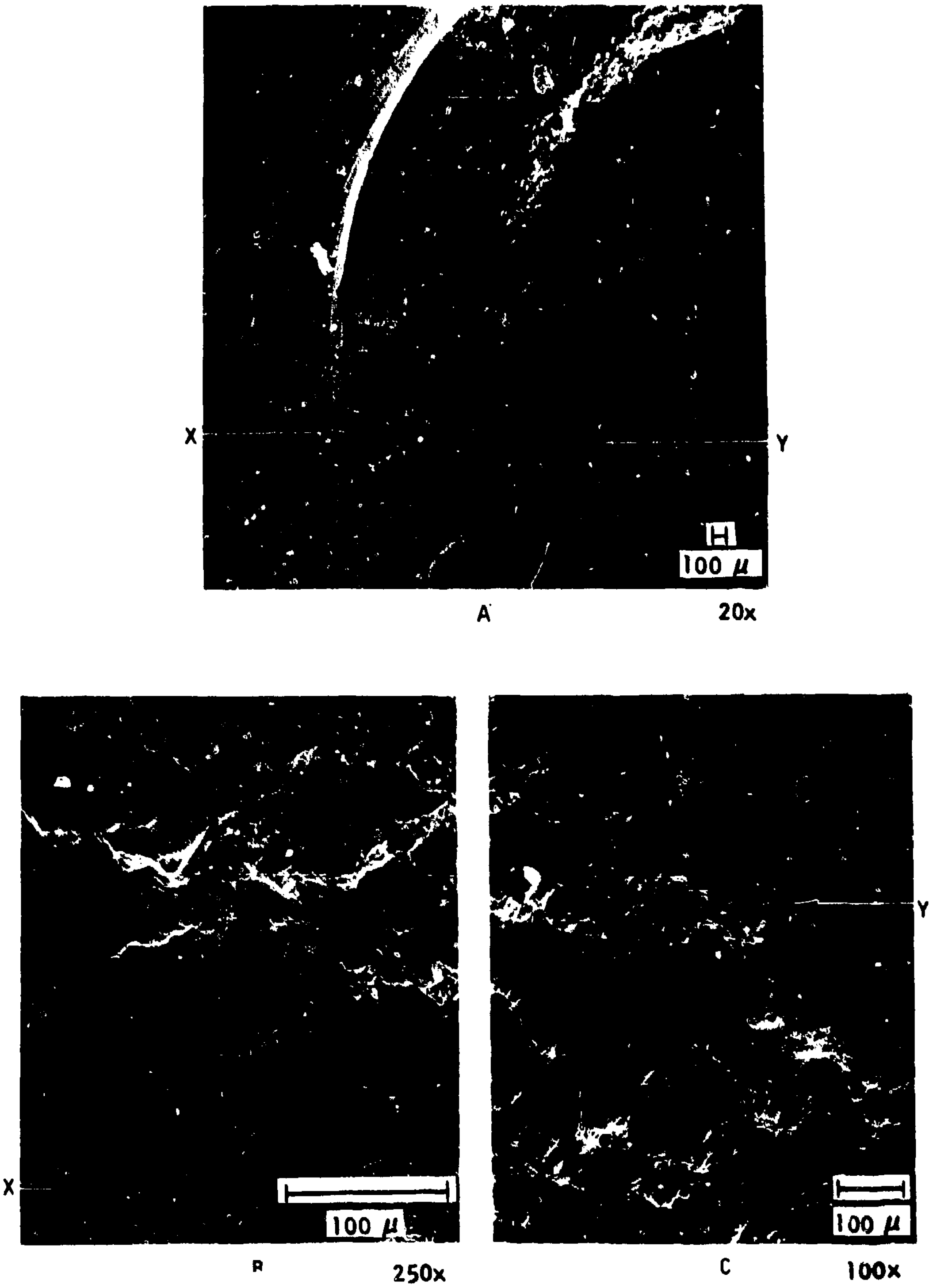

Figure 16. Electron Fractography of Haynes 188 Low-Cycle-Fatigue Specimen No. 9 Tested With Argon at 1450 F With 1.44% Strain Range

Electron fractographs of a Haynes 188 specimen tested with argon are contained in Fig. 16. Figure 16A is a low-magnification cross section of the specimen and Fig. 16B and 16C are higher magnification fractographs of regions in the cross section. X and Y locate the same features in the low- and high-magnification fractographs. Figure 16B shows a crack initiation site at the outside of the specimen with striations indicating inward crack growth. Figure 16C shows a ductile region at the inside surface. Other crack-initiation, striation regions were found at the outside, none at the inner surface. Thus, for this specimen tested with argon, cracks initiated at the outside surface and grew inward through the wall. As noted earlier, most of the low-cycle-fatigue specimens failed in the radii at the ends of the straight gage section because of the small stress concentration. Thus, with the same environment outside as inside, crack initiation would be expected to occur at the outside. Electron fractographs of a Haynes 188 specimen tested with $NH_3/N_2/H_2$ are presented in Fig. 17. Figure 17A and 17C are low-magnification cross sections of the specimen, and Fig. 17B and 17D are higher-magnification regions in the respective cross sections. X and Y locate the same features in the low- and high-magnification fractographs. Fractograph 17B shows striations proceeding from the inside surface, and 17D shows striations proceeding from the outside surface. Therefore, the effect of the $NH_3/N_2/H_2$ environment on Haynes 188 was sufficient to cause crack initiation at the inside surface, but not so large as to cause failure from the inside without initating any cracks on the outside surface. Thus, the fractography results correlate well with the somewhat reduced fatigue life of Haynes 188 in $NH_3/N_2/H_2$ compared to argon.

Electron fractographs of an Inconel 600 specimen tested with argon are contained in Fig. 18. Figure 18A is a low-magnification cross section of the specimen, and Fig. 18B and 18C are higher-magnification fractographs of regions in the cross section, and the respective regions are located in Fig. 18A. The fractograph in Fig. 18D was taken in the center of the specimen wall at a location clockwise from Fig. 18A at about the 4 o'clock position. Figure 18B shows the presence of fracture surface

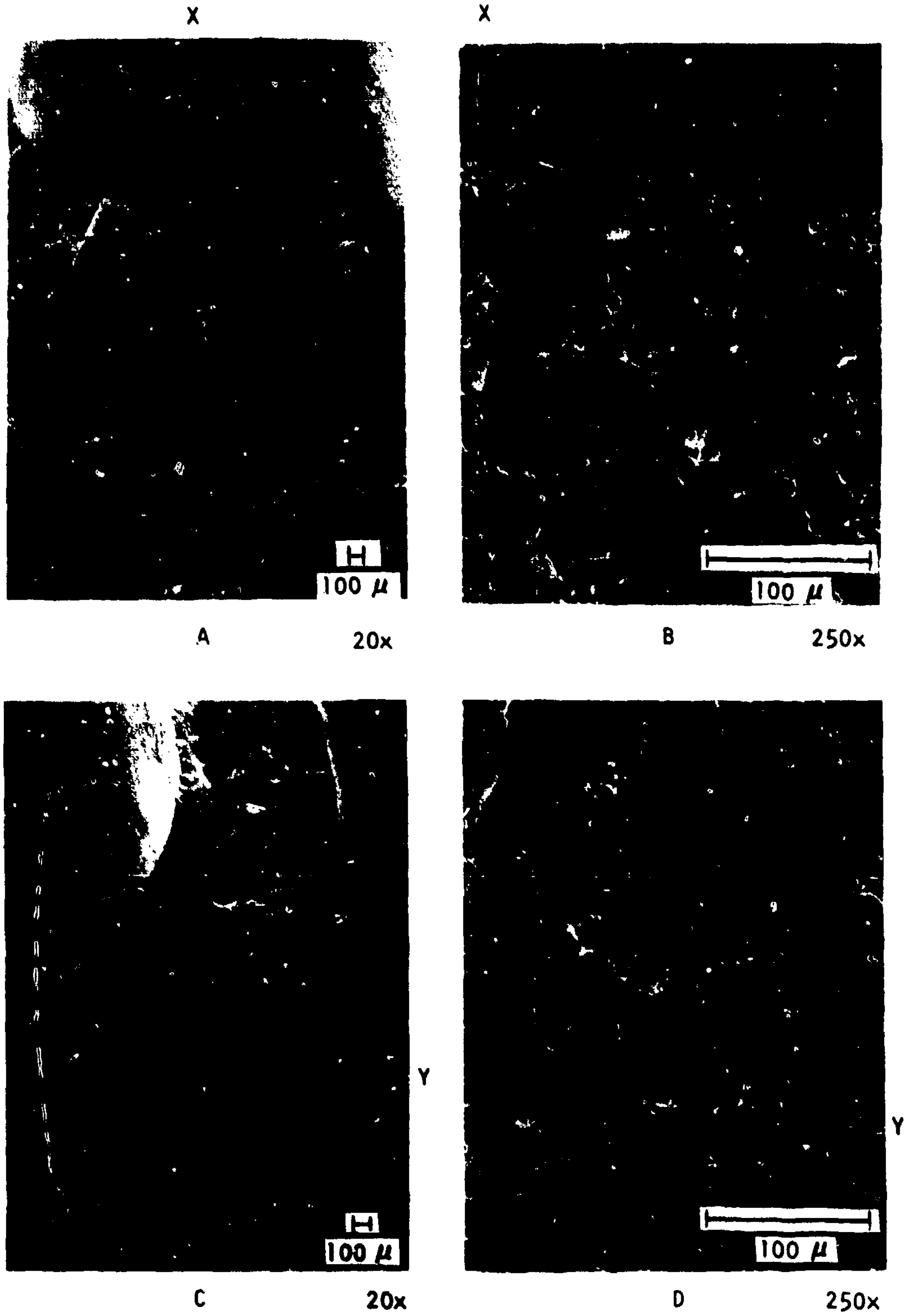

Figure 17. Electron Fractograph of Haynes 188 Low-Cycle-Fatigue Specimen No. 10 Tested With $NH_3/N_2/H_2$ at 1450 F With 1.48% Strain Range

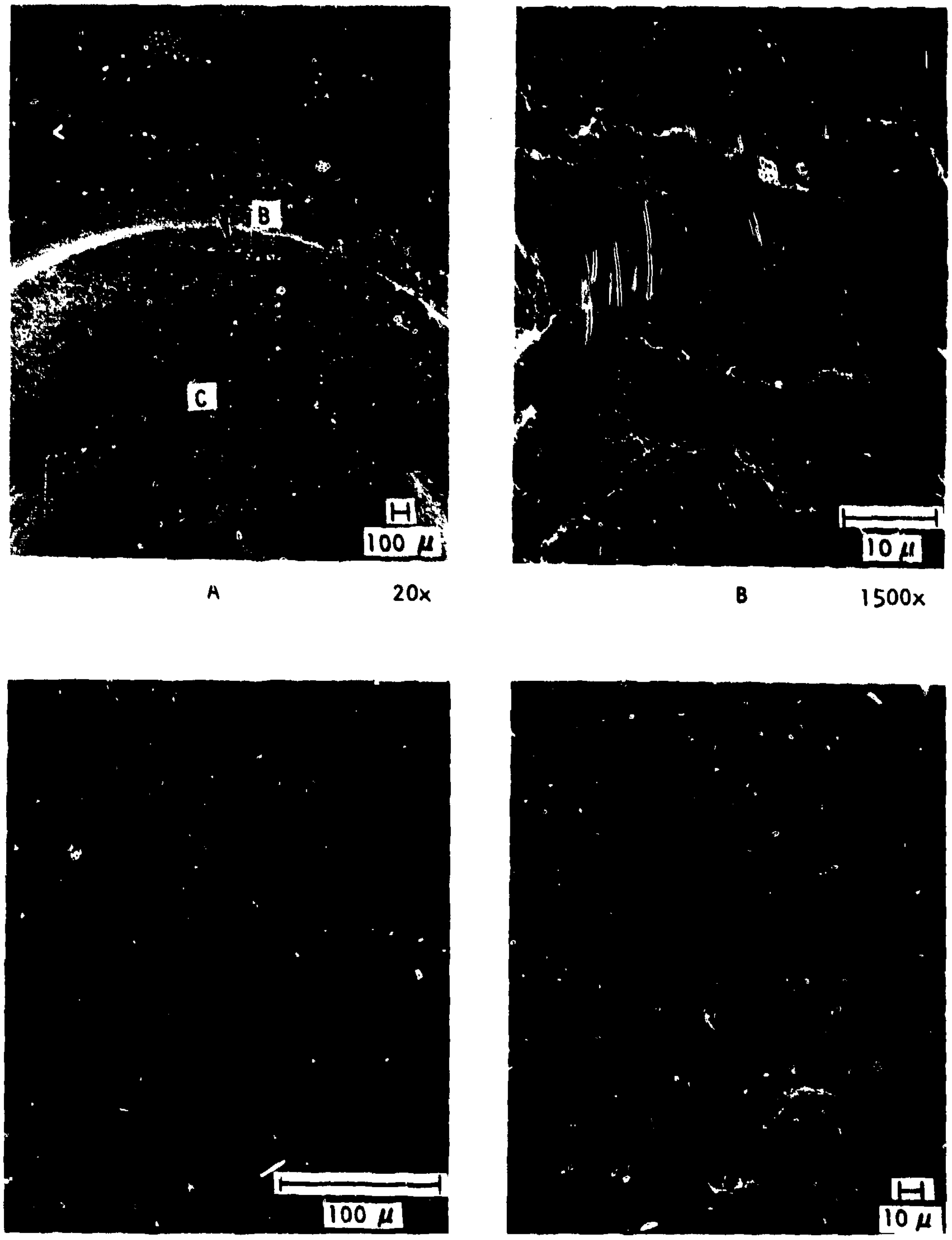

A 20x

B 1500x

C 250x

D 300x

Figure 18. Electron Fractography of Inconel 600 Low-Cycle-Fatigue Specimen No. 8 Tested With Argon at 1450 F With 1.50% Strain Range

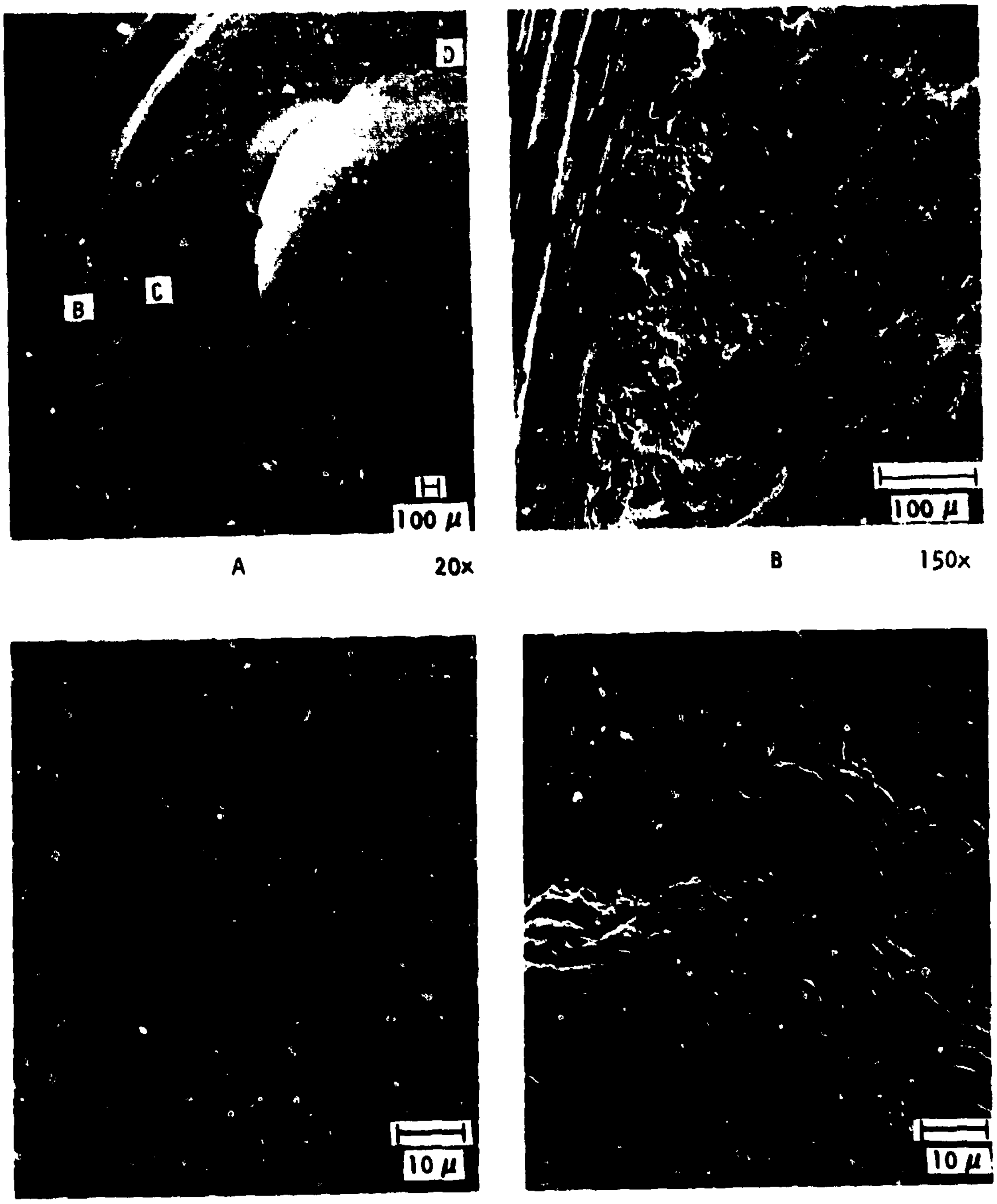

A 20x B 150x

C 1000x D 1000x

Figure 19. Electron Fractography of Inconel 600 Low-Cycle-Fatigue Specimen No. 10 With $NH_3/N_2/H_2$ at 1450 F With 1.48% Strain Range (The Dark Regions in B are Artifacts)

oxidation. This fractograph also shows the presence of striations that proceed from the outside of the specimen, which is at the top of Fig. 18B, through the wall. Figure 18C shows the shear fracture appearance of the shear lip at the inside surface. Figure 18D shows a ductile fracture of the long shear rupture type resulting from the formation of elongated dimples, with the direction of crack growth being from top to bottom, i.e., along, not through, the wall at the location identified above. Thus, in this Inconel 600 specimen, a crack initiated at the outside surface and proceeded through and along the wall to failure. Electron fractographs of an Inconel 600 specimen tested with $NH_3/N_2/H_2$ are presented in Fig. 19. The location of the higher-magnification Fig. 19B, C, and D fractographs are indicated on the low-magnification Fig. 19A cross section. Figure 19B shows a thin, very brittle appearing layer at the outside surface of the specimen. The reason for this brittle layer is not apparent, such a brittle appearance is not seen elsewhere, and no striations are contained within or emanate from the brittle layer. Figure 19C shows a typical ductile fracture inside the specimen wall. Figure 19D, and other fractographs not presented, show striations which proceed through the wall from the inside surface, which is toward the bottom of Fig. 19D. Thus, the effect of the $NH_3/N_2/H_2$ environment on Inconel 600 was sufficient to cause crack initiation at the inside surface as opposed to initiation at the outside with argon. These observations correlate with the lower fatigue life with $NH_3/N_2/H_2$ compared with argon for Inconel 600 tested at the higher strain range.

Electron fractographs of a Rene' 41 specimen tested with argon are contained in Fig. 20. Figure 20A is a fractograph at the outside surface. Relative to the low magnification cross section shown in Fig. 20D, the location of the region in Fig. 20A is at 12 o'clock. Figure 20B is a high-magnification fractograph of the region pointed out in Fig. 20A. Figure 20A and B show striations proceeding inward from the outside surface. Figure 20C shows a typical ductile fracture region which is approximately half way through the wall from the region shown in Fig. 20A. Figure 20D shows the bright ductile shear lip which was found around the

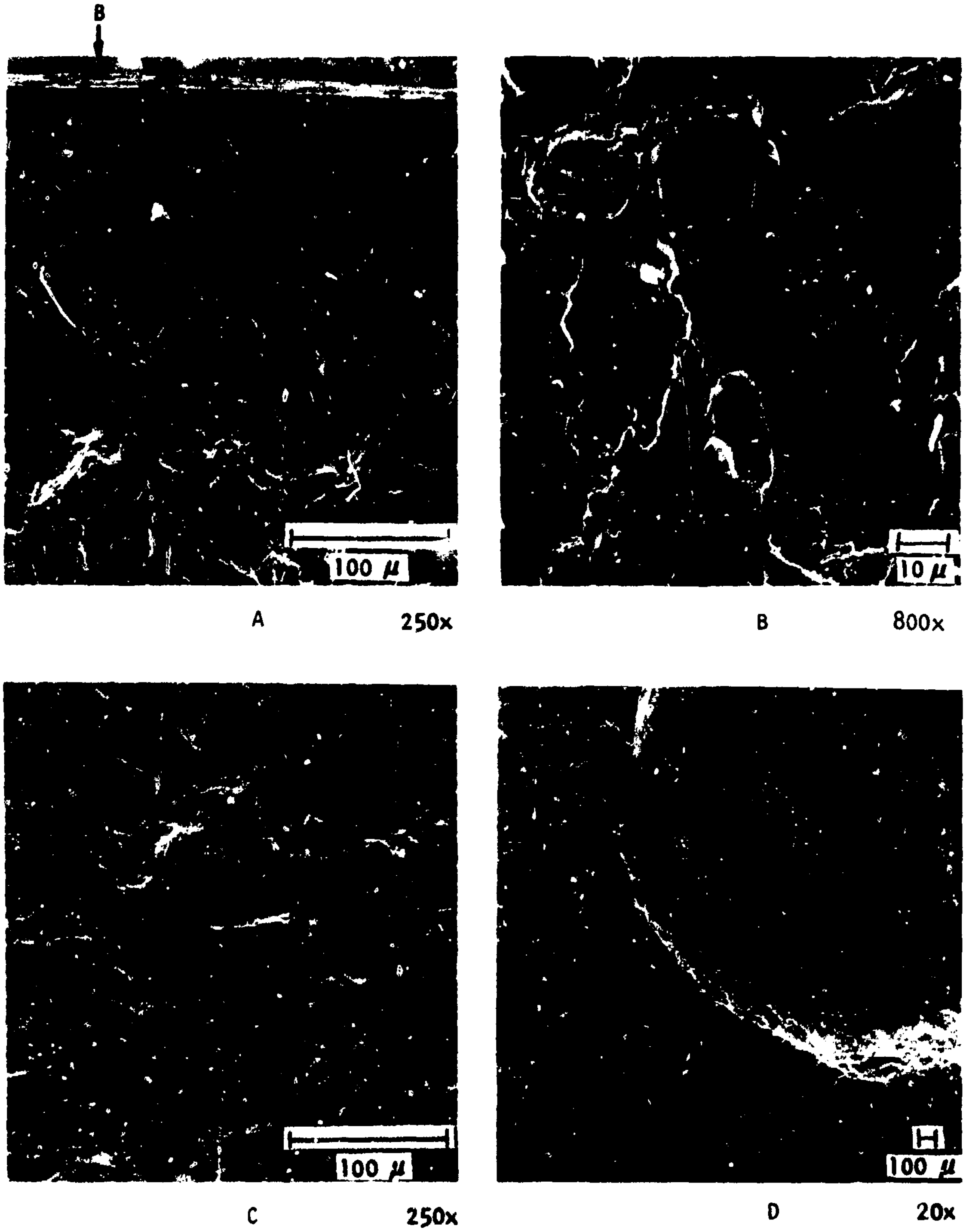

Figure 20. Electron Fractography of Rene' 41 Low-Cycle-Fatigue Specimen No. 4 Tested With Argon at 1450 F With 1.47% Strain Range

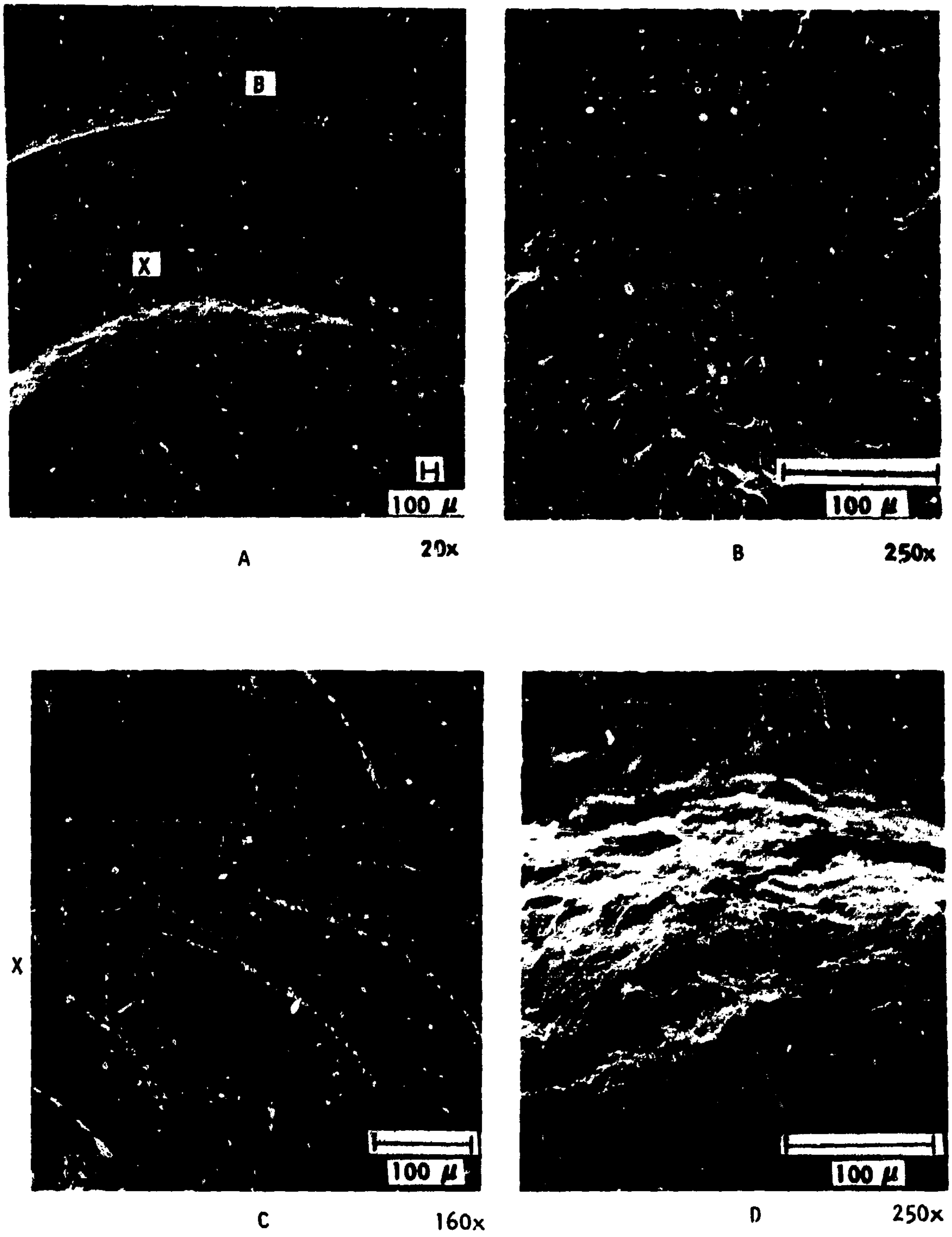

Figure 21. Electron Fractrography of Rene'41 Low-Cycle-Fatigue Specimen No. 6 With $NH_3/N_2/H_2$ at 1450 F With 1.50% Strain Range

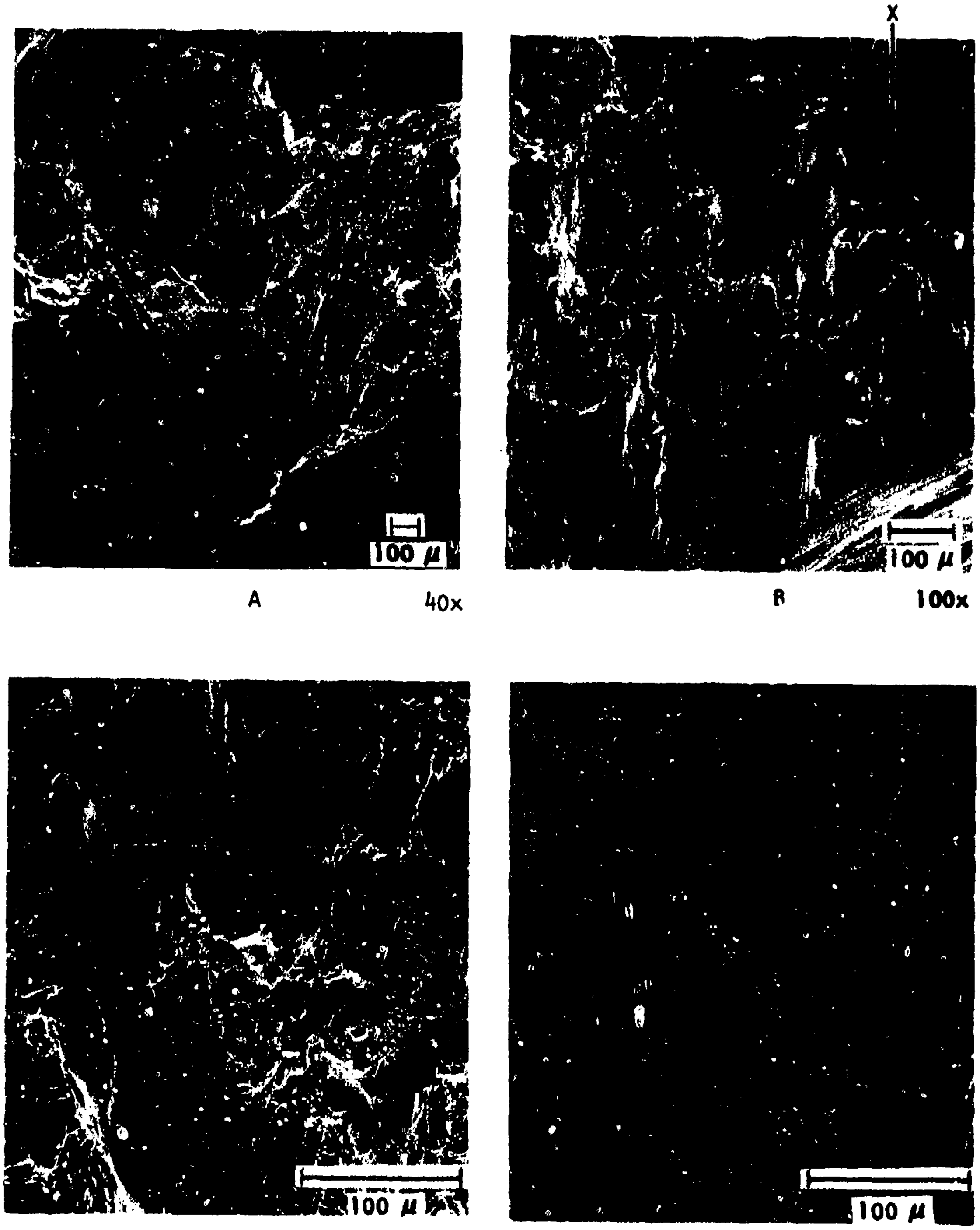

A 40x

B 100x

C 250x

D 250x

Figure 22. Electron Fractography of IN-100 Low-Cycle-Fatigue Specimen No. 9 Tested With Argon at 1450 F With 1.10% Strain Range

entire inside surface. Thus, the crack in the Rene' 41 specimen tested in argon initiated at the inside surface and grew through the wall. Electron fractographs of a Rene' 41 specimen tested with $NH_3/N_2/H_2$ are presented in Fig. 21. The Fig. 21A cross section shows the bright shear lip which extended around the inside of the specimen. The location of the region shown in Fig. 21B is pointed out in Fig. 21A. Figure 21B contains striations which are rather poorly defined. There are other locations around the specimen at which striations are seen proceeding from the outside surface inward. No striations were found at the inside surface. Figure 21C shows a typical ductile fracture at a region which can be located in Fig. 21A by the fracture feature identified by the X in both fractographs. Figure 21D shows a higher magnification of the ductile shear lip. A portion of the shear lip shown in Fig. 21D can be seen at the bottom of Fig. 21C. Thus, with $NH_3/N_2/H_2$ as well as with argon, cracks in low-cycle-fatigue-tested Rene' 41 specimens initiated at the outside surface and grew through the wall. This correlates with the fact that the low-cycle-fatigue life of Rene' 41 was essentially the same for the two environments.

Electron fractographs of an IN-100 specimen tested with argon are contained in Fig. 22. Figure 22A shows the typical overall brittle appearance of an IN-100 fracture. Figure 22B shows casting microporosity and features (noted by "X") which are believed due to carbides that were observed in the IN-100 microstructure by optical microscopy. Figure 22C shows a relatively ductile region in the center of the specimen wall. Figure 22D shows a region at the inside surface of quasi-cleavage mixed with some shear. No striations were found in this specimen, and a crack initiation site could not be identified. Electron fractographs of an IN-100 specimen tested with $NH_3/N_2/H_2$ are contained in Fig. 23. The locations of the higher-magnification, Fig. 23B, C, and D fractographs are indicated on the low-magnification Fig. 23A cross section. Figure 23B shows a very brittle region at the outside surface which may be where a crack initiated. Figure 23C shows a ductile region. Figure 23D shows a region of shear fracture at the inside surface. No striations were found in this specimen. The electron fractography results are not as

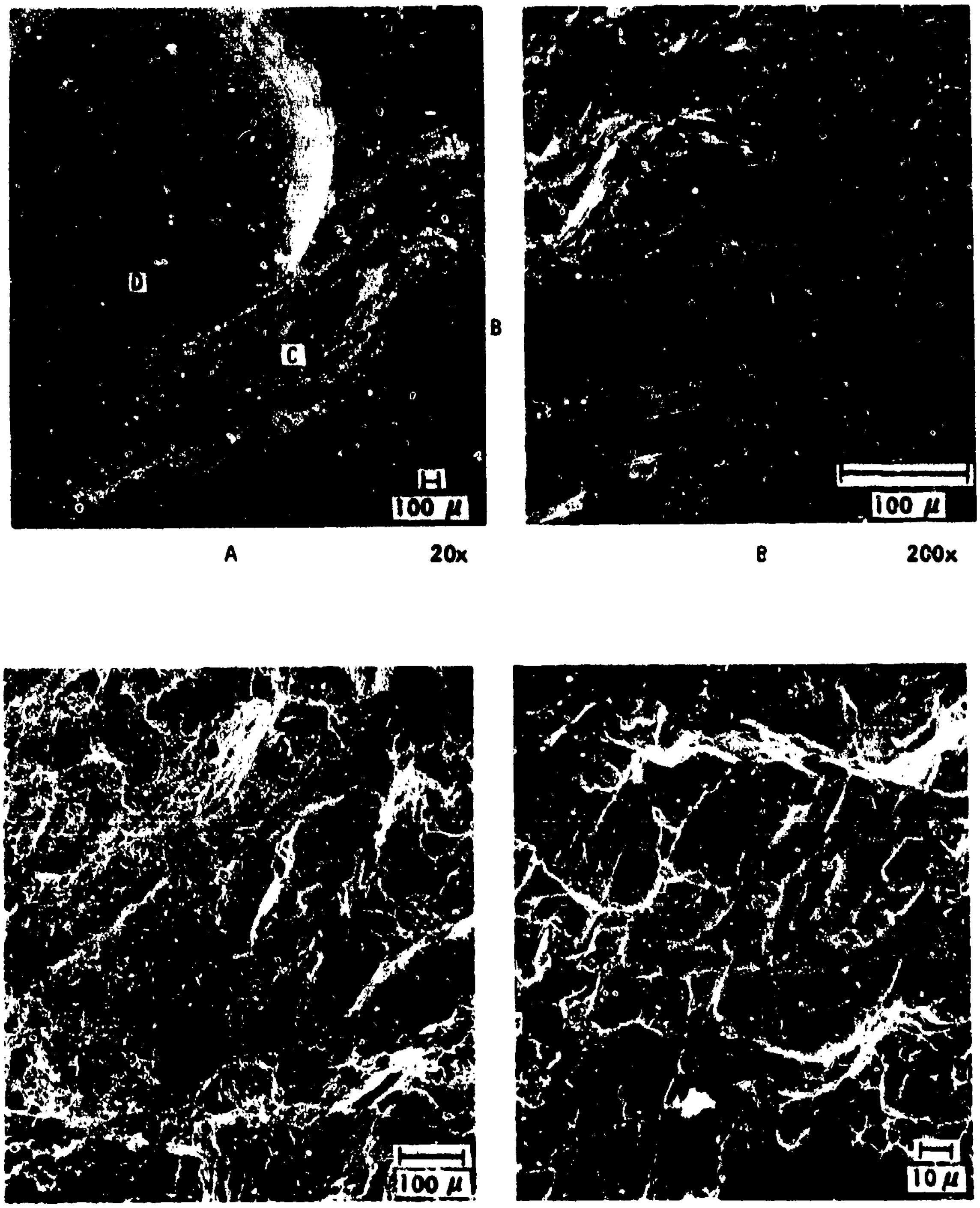

A 20x

B 200x

C 100x

D 500x

Figure 23. Electron Fractography of IN-100 Low-Cycle-Fatigue Specimen No. 1 Tested With $NH_3/N_2/H_2$ at 1450 F With 0.96% Strain Range

clear for IN-100 as for the other materials, but the fact that there was no significant difference in the fracture appearance between the specimen tested with argon and the specimen tested with $NH_3/N_2/H_2$, and the fact that the final shear failure occurred at the inside surface for both specimens, point to a lack of any environmental effect by the $NH_3/N_2/H_2$ environment. This conclusion agrees with the fact that the low-cycle-fatigue life of IN-100 was essentially the same in $NH_3/N_2/H_2$ as in argon.

CONCLUSIONS

The following conclusions are made as the result of the tests to determine the effect of $NH_3/N_2/H_2$ environments simulating APU system hydrazine decomposition products on the tensile properties and compressive low-cycle-fatigue properties of Haynes 188, Inconel 600, Rene' 41, and IN-100.

1. No significant effects of $NH_3/N_2/H_2$ environments on microstructures or tensile properties of any of the four alloys were found for specimens tested at 1450 or 1600 F, even following exposure periods up to 2 hours.
2. Low-cycle fatigue life was measurably reduced by exposure to $NH_3/N_2/H_2$ environments, compared to argon exposure, for Haynes 188 and Inconel 600 tested at 1450 F with compressive strain ranges of approximately 1.5% at a frequency of 0.5 Hz. At lower strain ranges, the low-cycle fatigue life of Haynes 188 also was slightly reduced by exposure to $NH_3/N_2/H_2$ environments, while for Inconel 600 the results are inconclusive because of some ambiguity in the argon baseline data. No consistent effects of $NH_3/N_2/H_2$ exposure on low-cycle fatigue life were observed for Rene' 41 or IN-100 specimens tested at 1450 F at a frequency of 0.5 Hz, even at the 1.5% strain range.
3. Electron fractography of specimens that were low-cycle fatigue tested at 1450 F, with compressive strain ranges of approximately 1.5% at a frequency of 0.5 Hz, showed that crack initiation in all four alloys occurred at the outer (argon exposed) surface, regardless of whether the specimens were internally pressurized with argon or $NH_3/N_2/H_2$. Cracks also initiated at the inner surface of Haynes 188 and Inconel 600 specimens that were internally pressurized with $NH_3/N_2/H_2$.
4. The results of a limited number of longer-cycle (0.1 Hz), low-cycle fatigue tests of Haynes 188, Inconel 600, and Rene' 41

specimens at 1450 F, with compressive strain ranges of approximately 1%, indicated that the longer cycle significantly reduced the low-cycle fatigue life in either of the environments. In the cases of Haynes 188 and Inconel 600, the reduction was greater for specimens exposed to $NH_3/N_2/H_2$. For Rene' 41 tested with the longer cycle, there was also some indication of a reduced low-cycle fatigue life with $NH_3/N_2/H_2$ compared with argon.

These conclusions pertain only to the test conditions used in this program. Greater effects of $NH_3/N_2/H_2$ environments might be found with longer hold times prior to tension tests or with tension cycles for the low-cycle-fatigue tests.

RECOMMENDATIONS

It is recommended that the effects of tensile strain cycles and extended exposure at peak strain in low-cycle fatigue tests be explored in future programs, since environmental effects may become more apparent under those conditions.

☆U.S.Government Printing Office: 1977 — 757-080/278